

Tetrapyridine/triphenyltriazine conjugated electron-transporters for low-power-consumption and highly stable phosphorescent OLEDs

*Tomoya Kawano¹, Hisahiro Sasabe^{*1,2,3}, Yu Saito¹, Yuhui Chen¹, Yuma Kori¹, Takeru Nakamura¹, Shoki Abe¹, Tomohiro Maruyama¹, Junji Kido^{1,2,3}*

¹Department of Organic Materials Science, Yamagata University, 4-3-16 Jonan, Yonezawa, Yamagata 992-8510, Japan, ²Research Center of Organic Electronics (ROEL), Yamagata University, 4-3-16 Jonan, Yonezawa, Yamagata 992-8510, Japan, and ³Frontier Center for Organic Materials (FROM), Yamagata University, 4-3-16 Jonan, Yonezawa, Yamagata 992-8510, Japan

General Information

Quantum chemical calculations were performed using the hybrid density functional theory (DFT), functional Becke and Hartree-Fock exchange, and Lee Yang and Parr correlation (B3LYP) as implemented in the Gaussian 09 program packages.^[1] Electrons were described by the Pople 6-31G(d) basis set for molecular structure optimization and single-point energy calculations, respectively. Differential scanning calorimetry (DSC) was performed using a Perkin-Elmer Diamond DSC Pyris instrument under nitrogen atmosphere at a heating rate of 10°C min⁻¹. Thermogravimetric analysis (TGA) was undertaken using a SEIKO EXSTAR 6000 TG/DTA 6200 unit under nitrogen atmosphere at a heating rate of 10°C min⁻¹. ¹H-NMR and ¹³C-NMR spectra were recorded on JEOL 400, 500, 600 spectrometers. Mass spectra were obtained using a JEOL JMS-K9 mass spectrometer and a Waters SQD2 mass spectrometer with atmospheric pressure solid analysis probe (ASAP). UV-Vis spectra was measured using a Shimadzu UV-3150 UV-vis-NIR spectrophotometer. Photoluminescence spectra were measured using a FluroMax-2 (Jobin-Yvon-Spex) luminescence spectrometer. The ionization potential (I_p) was determined using a Sumitomo Heavy Industries, Ltd PYS-201 in vacuum ($\sim 10^{-3}$ Pa).^[2] Photoluminescence quantum yield were measured using a Hamamatsu C11347 absolute PL quantum yield spectrometer with an integral sphere at an excitation wavelength of each sample.

[1] *Gaussian 09*, Revision D.01, M. J. Frisch, G. W. Trucks, H. B. Schlegel, G. E. Scuseria, M. A. Robb, J. R. Cheeseman, G. Scalmani, V. Barone, B. Mennucci, G. A. Petersson, H. Nakatsuji, M. Caricato, X. Li, H. P. Hratchian, A. F. Izmaylov, J. Bloino, G. Zheng, J. L. Sonnenberg, M. Hada, M. Ehara, K. Toyota, R. Fukuda, J. Hasegawa, M. Ishida, T. Nakajima, Y. Honda, O. Kitao, H. Nakai, T. Vreven, J. A. Montgomery, Jr., J. E. Peralta, F. Ogliaro, M. Bearpark, J. J. Heyd, E. Brothers, K. N. Kudin, V. N. Staroverov, R. Kobayashi, J. Normand, K. Raghavachari, A. Rendell, J. C. Burant, S. S. Iyengar, J. Tomasi, M. Cossi, N. Rega, J. M. Millam, M. Klene, J. E. Knox, J. B. Cross, V. Bakken, C. Adamo, J. Jaramillo, R. Gomperts, R. E. Stratmann, O. Yazyev, A. J. Austin, R. Cammi, C. Pomelli, J. W. Ochterski, R. L. Martin, K. Morokuma, V. G. Zakrzewski, G. A. Voth, P. Salvador, J. J. Dannenberg, S. Dapprich, A. D. Daniels, Ö. Farkas, J. B. Foresman, J. V. Ortiz, J. Cioslowski, and D. J. Fox, Gaussian, Inc., Wallingford CT, 2013.

[2] H. Ishii, D. Tsunami, T. Suenaga, N. Sato, Y. Kimura, M. Niwano, *J. Surf. Sci. Soc. Jpn.* 2007, 28, 264.

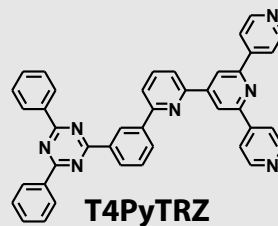
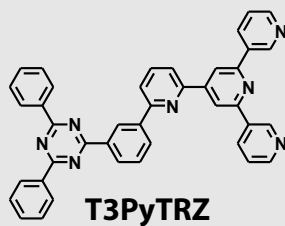
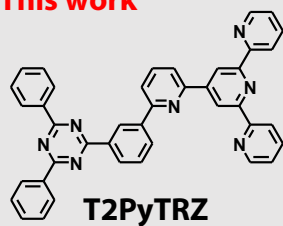
Device Fabrication

The substrates were cleaned with ultra-purified water and organic solvents, and then dry-cleaned for 20 minutes by exposure to UV–ozone. The organic layers were deposited onto the ITO substrates under the vacuum ($=10^{-5}$ Pa), successively. Al was patterned using a shadow mask with an array of $2\text{ mm} \times 2\text{ mm}$ openings without breaking the vacuum ($=10^{-5}$ Pa). The electroluminescent (EL) were taken using an optical multichannel analyzer Hamamatsu Photonics PMA-11. The current density–voltage and luminance–voltage characteristics were measured by using a Keithley source measure unit 2400 and a Minolta CS2000 luminance meter, respectively.

Table S1. Summary of device performances in green phosphorescent OLEDs.

ETL	V_{on}/V_{1000} (V)	$PE_{\text{max}}/PE_{1000}$ (lm/W)	$EQE_{\text{max}}/EQE_{1000}$ (%)	LT ₅₀ at 1000 cd/m ²	Ref
T3PyTRZ	2.18/2.88	115/88.0	23.0/22.5	31662 h (251 h@25 mA/cm²)	This work
T2PyTRZ	2.68/3.79	105/65.5	26.0/21.9	13272 h (155 h@25 mA/cm²)	This work
T4PyTRZ	2.74/3.77	98.3/72.2	25.0/24.0	15290 h (120 h@25 mA/cm²)	This work
DPPyA	2.35/-	107/—	28.2/—	not reported	1
B3PyMPM	2.9/3.14	133/107	29/26	not reported	2
s2TPy	3.14/5.96	—/41.0	—/21.7	18158 h (171 h@25 mA/cm ²)	3
s3TPy	2.76/4.13	—/61.3	—/22.5	17216 h (219 h@25 mA/cm ²)	3
s4TPy	2.83/4.18	—/64.5	—/24.0	19345 h (172 h@25 mA/cm ²)	3
B2PyPC	3.09/5.70	—/44.1	—/12.2	8080 h (221 h@25 mA/cm ²)	4
B3PyPC	2.49/3.61	—/66.8	—/18.6	10814 h (170 h@25 mA/cm ²)	4
B4PyPC	2.38/3.86	—/64.1	—/17.8	18290 h (268 h@25 mA/cm ²)	4
27-TPSF	2.4/—	94.7/82.0	24.5/24.2	6804 h (121 h@10000 cd/m ²)	5
22-TPSF	2.6/—	88.7/33.1	22.9/19.1	3092 h (55 h@10000 cd/m ²)	5
27m-TPSF	2.3/—	88.0/70.0	20.4/19.4	4330 h (77 h@10000 cd/m ²)	6
3-4PySF	2.6/—	83.6/47.9	20.5/20.1	not reported	7
4-4PySF	2.8/—	62.7/31.1	18.3/17.9	not reported	7
4oTPSF	2.23	97.8/65.6	19.4/18.4	5680 h (101 h@10000 cd/m ²)	8
T3PySS	2.2/—	—/—	12.0/—	1100 h (LT ₉₀ @2000 cd/m ²)	9
T3PySO	2.4/—	—/—	12.6/—	580 h (LT ₉₀ @2000 cd/m ²)	9
D3PySF	2.5/—	—/—	13.1/—	559 h (LT ₉₀ @2000 cd/m ²)	9

This work



Previous work

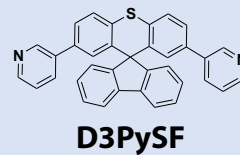
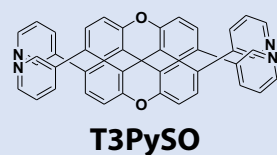
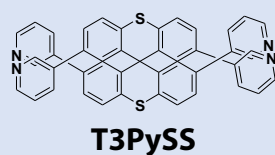
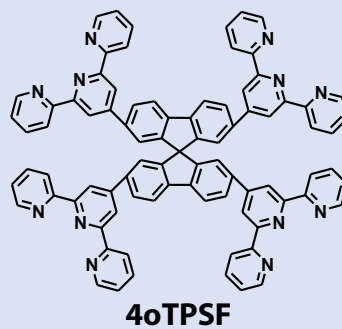
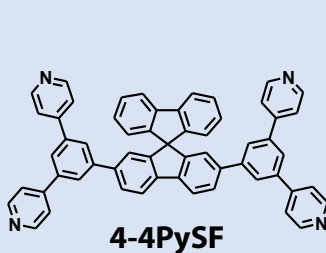
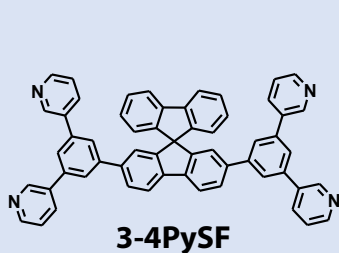
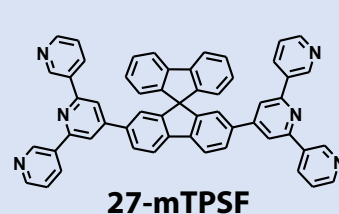
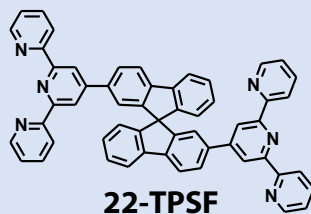
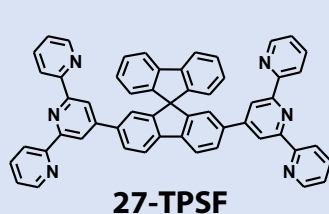
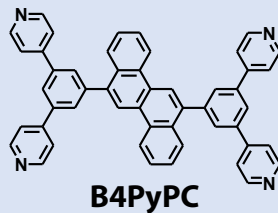
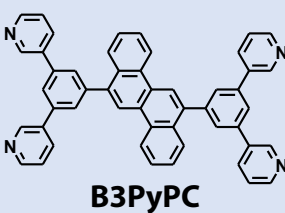
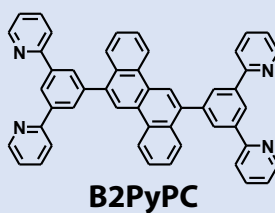
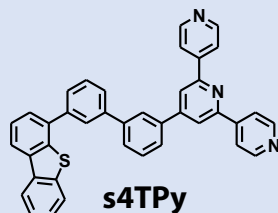
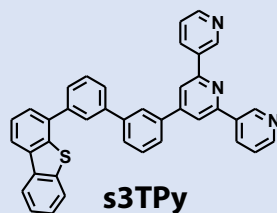
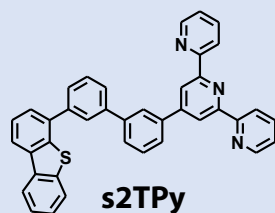
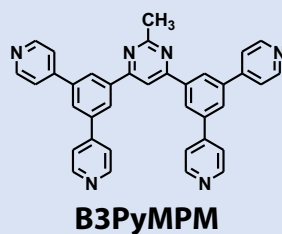
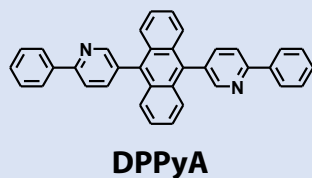


Chart S1. Chemical structures of ETLs.

References

- [1] D. Zhang, J. Qiao, D. Zhang, L. Duan, *Adv. Mater.* **2017**, *29*, 1702847.
- [2] D. Tanaka, H. Sasabe, Y.-J. Li, S.-J. Su, T. Takeda, J. Kido, *Jpn. J. Appl. Phys.* **2007**, *46*, L10.
- [3] T. Maruyama, H. Sasabe, Y. Watanabe, T. Owada, R. Yoshioka, Y. Saito, T. Kawano, J. Kido, *Chem. Lett.* **2021**, *50*, 534.
- [4] T. Watanabe, H. Sasabe, T. Owada, T. Maruyama, Y. Watanabe, H. Katagiri, J. Kido, *Chem. Lett.* **2019**, *48*, 457.
- [5] M. Bian, Y. Wang, X. Guo, F. Lv, Z. Chen, L. Duan, Z. Bian, Z. Liu, H. Geng, L. Xiao, *J. Mater. Chem. C*, **2018**, *6*, 10276.
- [6] X. Guo, M. Bian, F. Lv, Y. Wang, Z. Zhao, Z. Bian, B. Qu, L. Xiao, Z. Chen, *J. Mater. Chem. C*, **2019**, *7*, 11581-11587.
- [7] X. Guo, F. Lv, Z. Zhao, J. Gu, B. Qu, L. Xiao, Z. Chen, *Org. Electron.* **2020**, *77*, 105498.
- [8] X. Guo, Z. Tang, W. Yu, Y. Wang, Z. Zhao, J. Gu, Z. Liu, B. Qu, L. Xiao, Z. Chen, *Org. Electron.* **2021**, *89*, 106048.
- [9] K. Duan, Y. Zhu, Z. Liu, D. Wang, C. Deng, S. Niu, T. Tsuboi, Q. Zhang, *Chem. Eng. J.* **2022**, *429*, 132215.

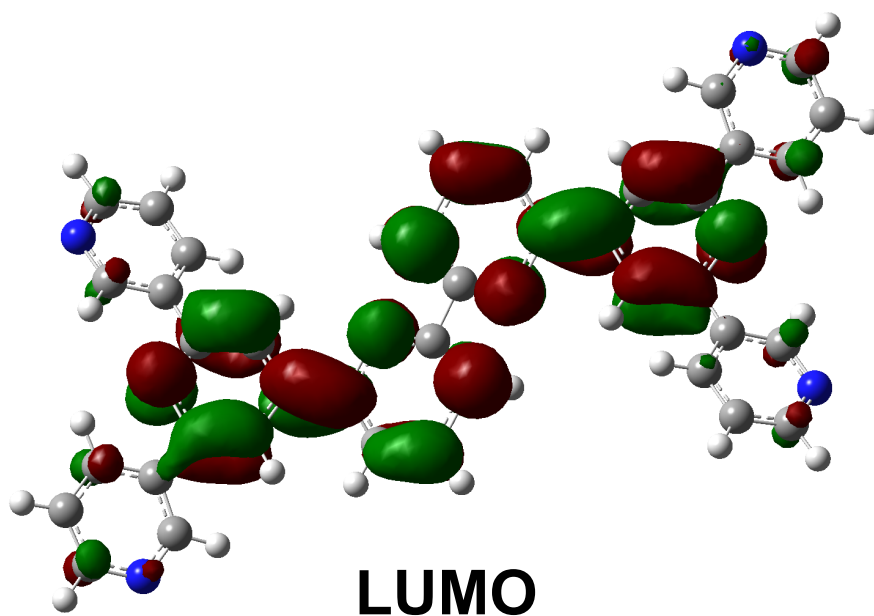
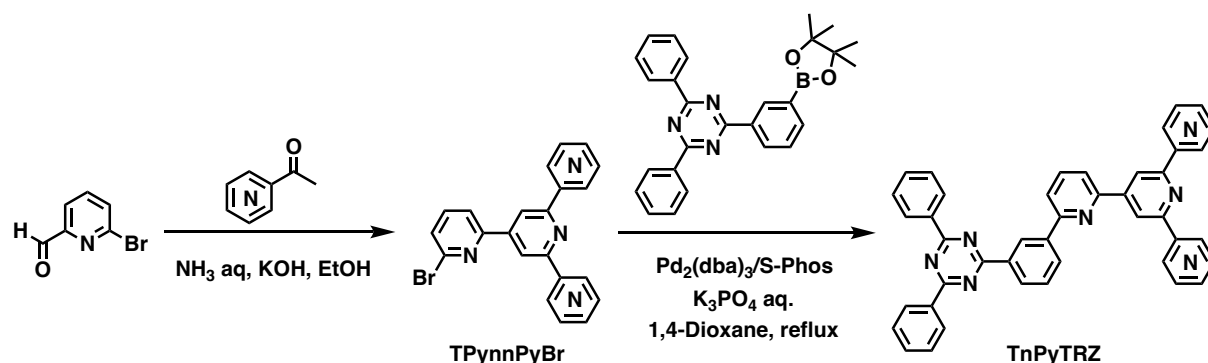


Figure S1. The electron cloud distributions of LUMO on 6,6'-BPY3TPY.



Scheme S1. Synthetic route of **TnPyTRZ** derivatives.

A mixture of 6-bromo-2-pyridinecarboxaldehyde (5.0 g, 26.9 mmol), 2-acetylpyridine (5.85 mL, 52.2 mmol), KOH (1.5 g, 20.2 mmol), ethanol (201 mL), and 28% aqueous NH_3 (136 mL) were stirred at ambient temperature for 25 hours. The precipitate was filtered, washed with water followed by ethanol, and recrystallization from toluene to give **TPy22PyBr** (2.49 g, 23.8%) as a white solid; $^1\text{H-NMR}$ (400 MHz, CDCl_3) δ 9.04 (s, 2H), 8.76 (d, $J = 4.4$ Hz, 2H), 8.67 (d, $J = 8.0$ Hz, 2H), 8.04 (d, $J = 8.0$ Hz, 1H), 7.92-7.87 (m, 2H), 7.70 (t, $J = 8.0$ Hz, 1H), 7.55 (d, $J = 8.4$ Hz, 1H), 7.39-7.36 (m, 2H) ppm; $^{13}\text{C-NMR}$ (151 MHz, CDCl_3) δ 156.4, 156.0, 149.8, 149.4, 149.0, 148.6, 147.0, 142.5, 139.1, 136.9, 128.0, 123.6, 121.7, 121.1, 120.1, 118.6 ppm; MS (ASAP): m/z 389 $[\text{M}+\text{H}]^+$.

Other **TPynnPyBr** derivatives were prepared according to the similar method.

TPy33PyBr (13.2%) as a white solid: $^1\text{H-NMR}$ (400 MHz, CDCl_3) δ 9.43 (d, $J = 2.4$ Hz, 2H), 8.72 (dd, $J = 4.8, 1.6$ Hz, 2H), 8.56-8.53 (m, 2H), 8.35 (s, 2H), 7.92 (d, $J = 7.6$ Hz, 1H), 7.76 (t, $J = 7.6$ Hz, 1H), 7.61 (d, $J = 8.0$ Hz, 1H), 7.50-7.46 (m, 2H) ppm; $^{13}\text{C-NMR}$ (151 MHz, CDCl_3) δ 155.8, 155.5, 150.6, 150.2, 149.7, 148.5, 147.1, 142.8, 139.4, 135.1, 134.8, 134.4, 134.1, 123.9, 123.3, 119.8, 117.5, 117.1, 116.7, 116.4 ppm; MS (ASAP): m/z 389 $[\text{M}+\text{H}]^+$.

TPy44PyBr (14.3%) as a white solid: $^1\text{H-NMR}$ (400 MHz, CDCl_3) δ 8.82-8.81 (m, 4H), 8.43 (s, 2H), 8.13-8.11 (m, 4H), 7.92 (d, $J = 7.6$ Hz, 1H), 7.76 (t, $J = 7.6$ Hz, 1H), 7.63 (d, $J = 8.4$ Hz, 1H) ppm; $^{13}\text{C-NMR}$ (151 MHz, CDCl_3) δ 155.6, 155.2, 151.2, 150.6, 150.0, 147.3, 145.7, 142.9, 139.5, 121.2, 119.8, 118.7 ppm; MS (ASAP): m/z 389 $[\text{M}+\text{H}]^+$.

Synthesis of T2PyTRZ:

TPy22PyBr (0.78 g, 2.0 mmol), **TRZ-Bpin** (1.04 g, 2.4 mmol), 1,4-dioxane 43 mL, and K_3PO_4 (3.74 g, 17.6 mmol) in 13 mL H_2O were added to a round bottom flask. Then, nitrogen bubbled through the mixture for 1 hour. Then, $\text{Pd}_2(\text{dba})_3$ (0.037 g, 0.040 mmol) and S-Phos (0.033 g,

0.080 mmol) was added and the resultant mixture was stirred 18 hours at reflux temperature under N₂ flow. The precipitate was filtered, and washed with water and MeOH. The resulting solid was purified by chromatography on the silica gel (eluent: chloroform/ methanol = 100:0 to 100:10 v/v). Repetitive recrystallization from ethanol/toluene mixture afforded **T2PyTRZ** (1.02 g, 83.2%) as a white solid: ¹H-NMR (400 MHz, CDCl₃) δ 9.54 (t, J = 1.6 Hz, 1H), 9.28 (s, 2H), 8.90-8.88 (m, 1H), 8.83-8.81 (m, 4H), 8.72-8.70 (m, 4H), 8.61-8.59 (m, 1H), 8.12 (dd, J = 6.8, 2.0 Hz, 1H), 8.06-8.00 (m, 2H), 7.92-7.87 (m, 2H), 7.77 (t, J = 8.0 Hz, 1H), 7.62-7.57 (m, 2H), 7.55-7.51 (m, 4H), 7.36-7.33 (m, 2H) ppm; MS (ASAP): m/z 618 [M+H]⁺. Anal. Calcd for C₄₁H₂₇N₇: C, 79.72; H, 4.41; N, 15.87%. Found: C, 79.70; H, 4.38; N, 15.97%.

Other **T_nPyTRZ** derivatives were prepared according to the similar method.

T3PyTRZ (75.3%) as a white solid: ¹H-NMR (400 MHz, CDCl₃) δ 9.51-9.49 (m, 3H), 8.92 (d, J = 8.4 Hz, 1H), 8.81 (d, J = 7.6 Hz, 4H), 8.71-8.70 (m, 2H), 8.59-8.52 (m, 5H), 8.11-8.06 (m, 2H), 8.00-7.99 (m, 1H), 7.80 (t, J = 8.0 Hz, 1H), 7.61 (t, J = 7.2 Hz, 2H), 7.55 (t, J = 7.2 Hz, 4H), 7.44-7.41 (m, 2H) ppm; MS (ASAP): m/z 618 [M+H]⁺. Anal. Calcd for C₄₁H₂₇N₇: C, 79.72; H, 4.41; N, 15.87%. Found: C, 79.78; H, 4.03; N, 15.89%

T4PyTRZ (80.6%) as a white solid: ¹H-NMR (400 MHz, CDCl₃) δ 9.56 (t, J = 1.6 Hz, 1H), 8.94-8.91 (m, 1H), 8.83-8.81 (m, 4H), 8.75 (dd, J = 4.6, 1.2 Hz, 4H), 8.68 (s, 2H), 8.48-8.45 (m, 1H), 8.17-8.16 (m, 4H), 8.09-8.08 (m, 2H), 8.01-7.99 (m, 1H), 7.80 (t, J = 7.6 Hz, 1H), 7.64-7.59 (m, 2H), 7.56-7.52 (m, 4H) ppm; MS (ASAP): m/z 618 [M+H]⁺. Anal. Calcd for C₄₁H₂₇N₇: C, 79.72; H, 4.41; N, 15.87%. Found: C, 79.73; H, 4.18; N, 15.92%.

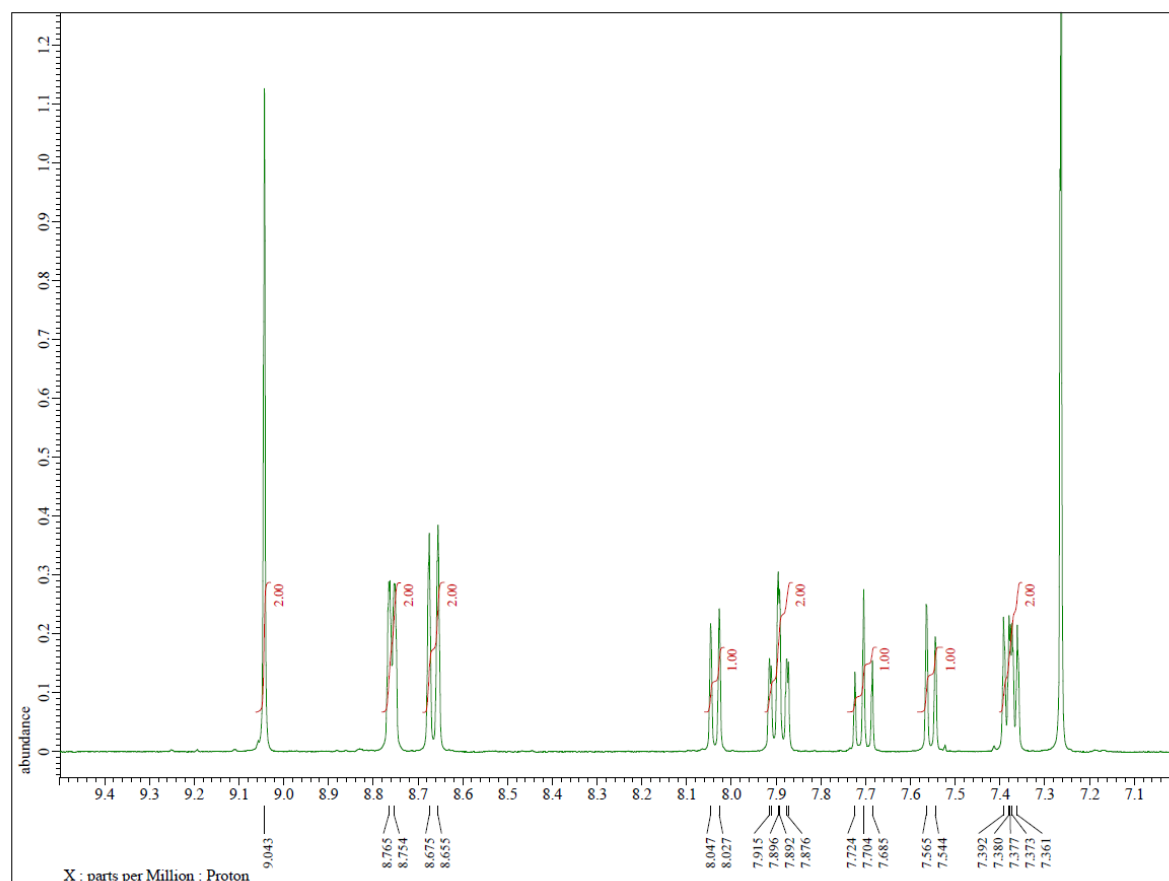
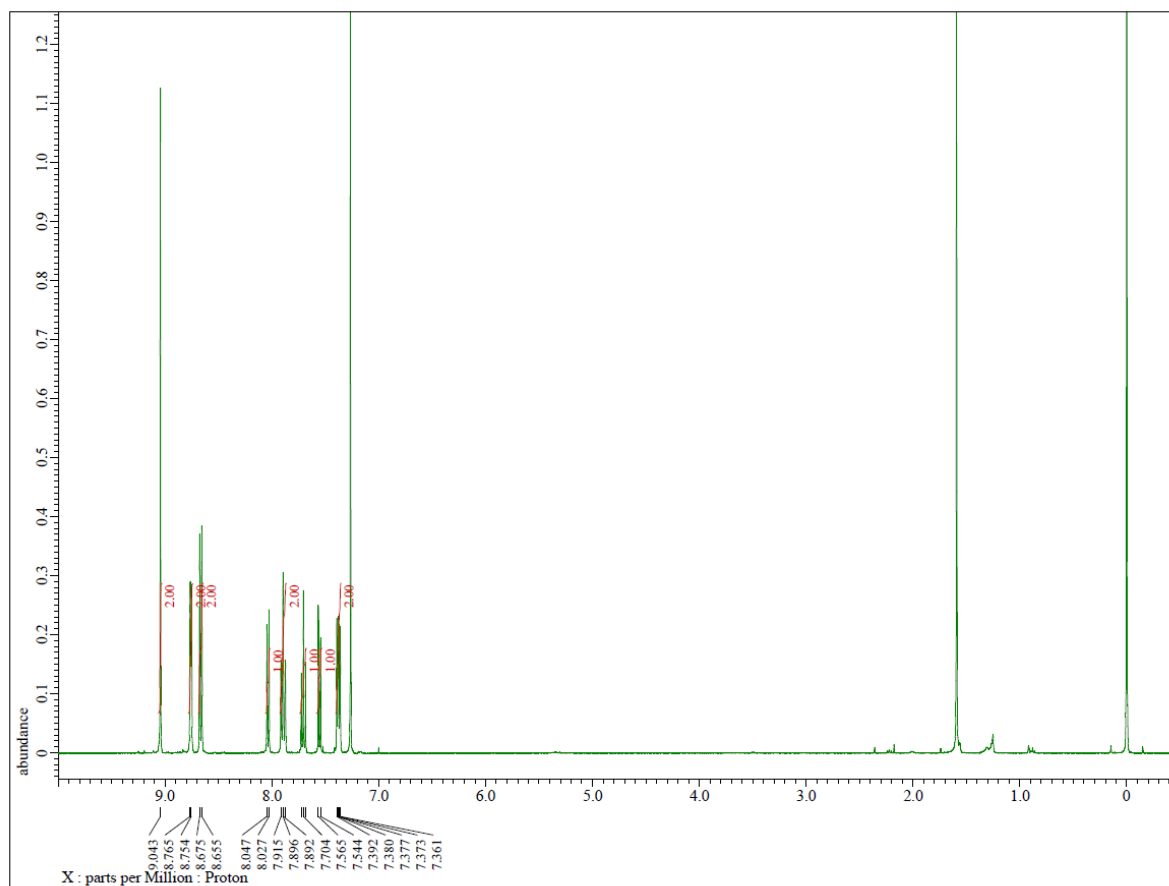


Figure S2. $^1\text{H-NMR}$ spectrum of **TPy22PyBr** (400 MHz, CDCl_3 , @R.T.)

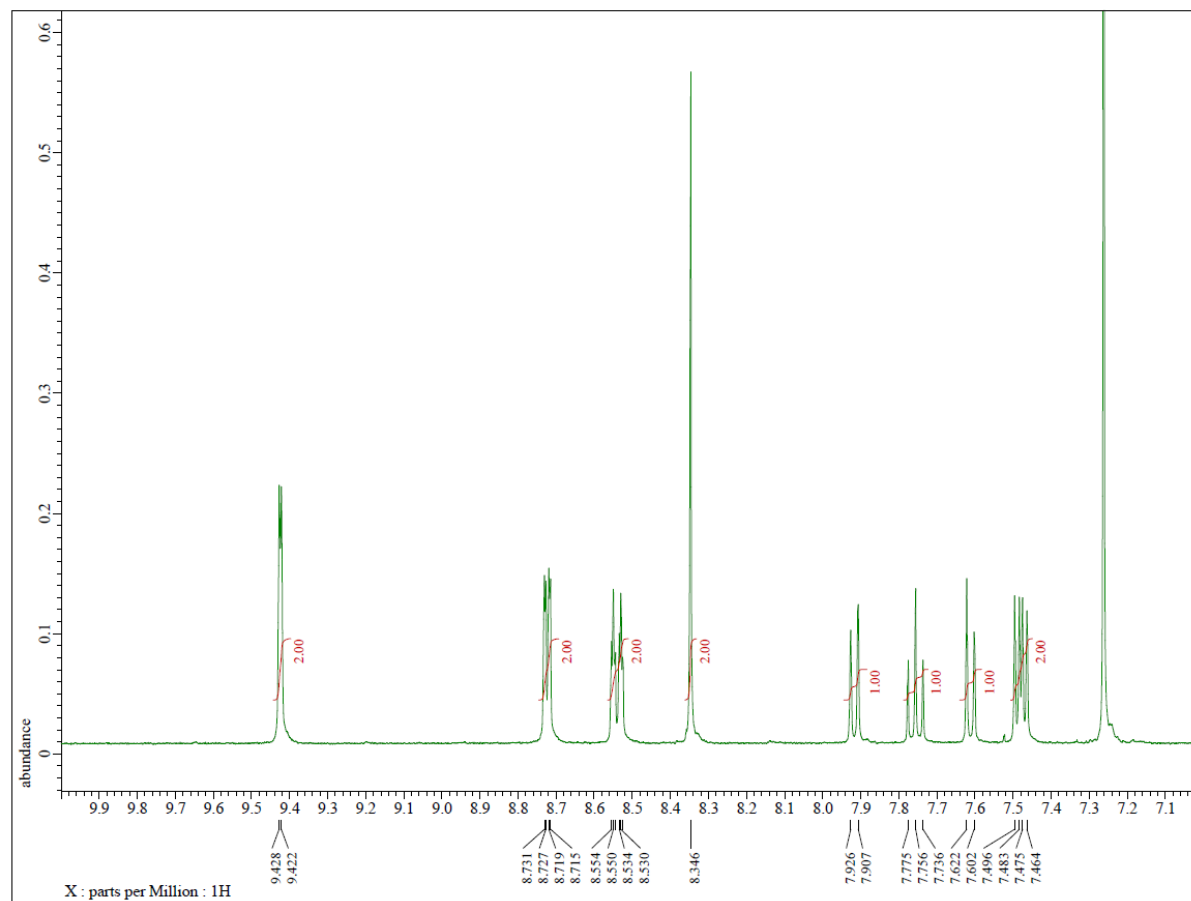
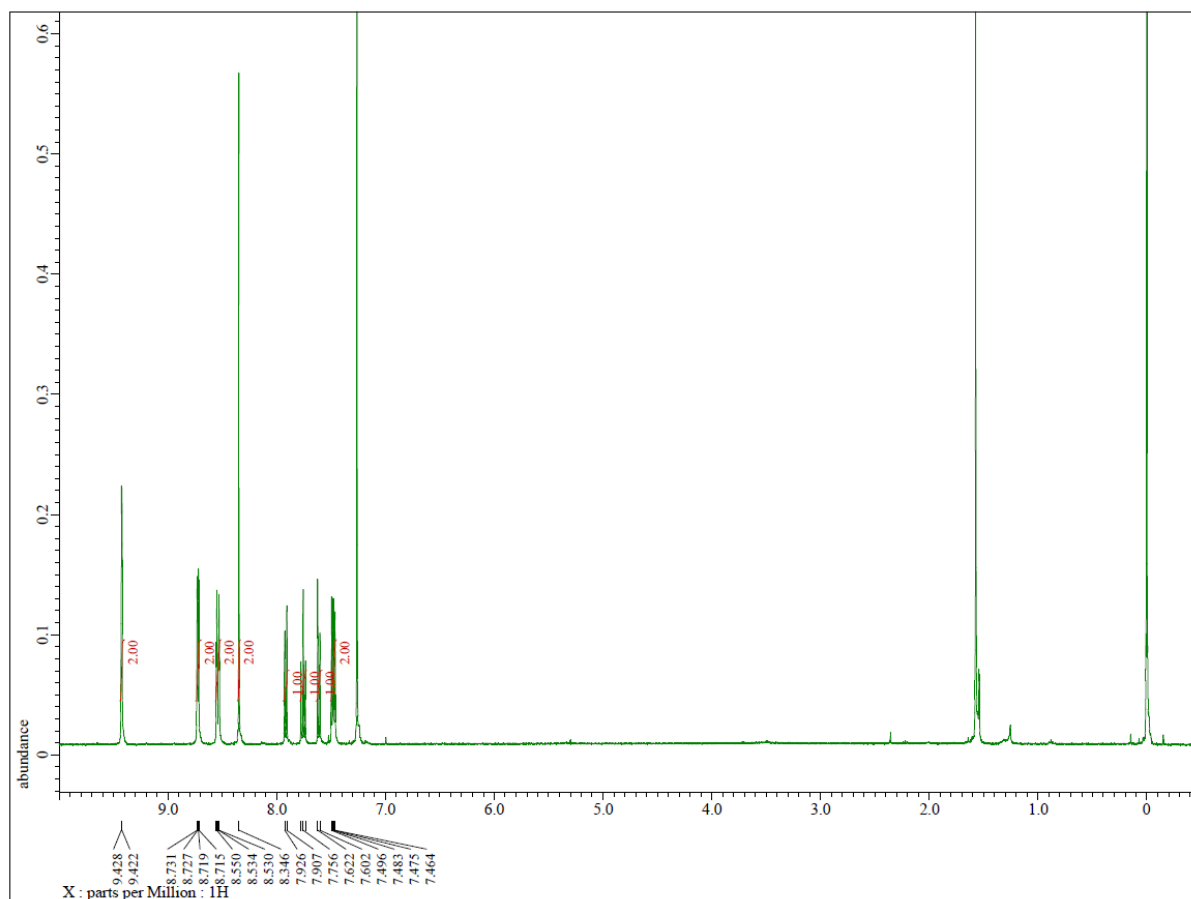


Figure S3. ^1H -NMR spectrum of TPy33PyBr (400 MHz, CDCl_3 , @R.T.)

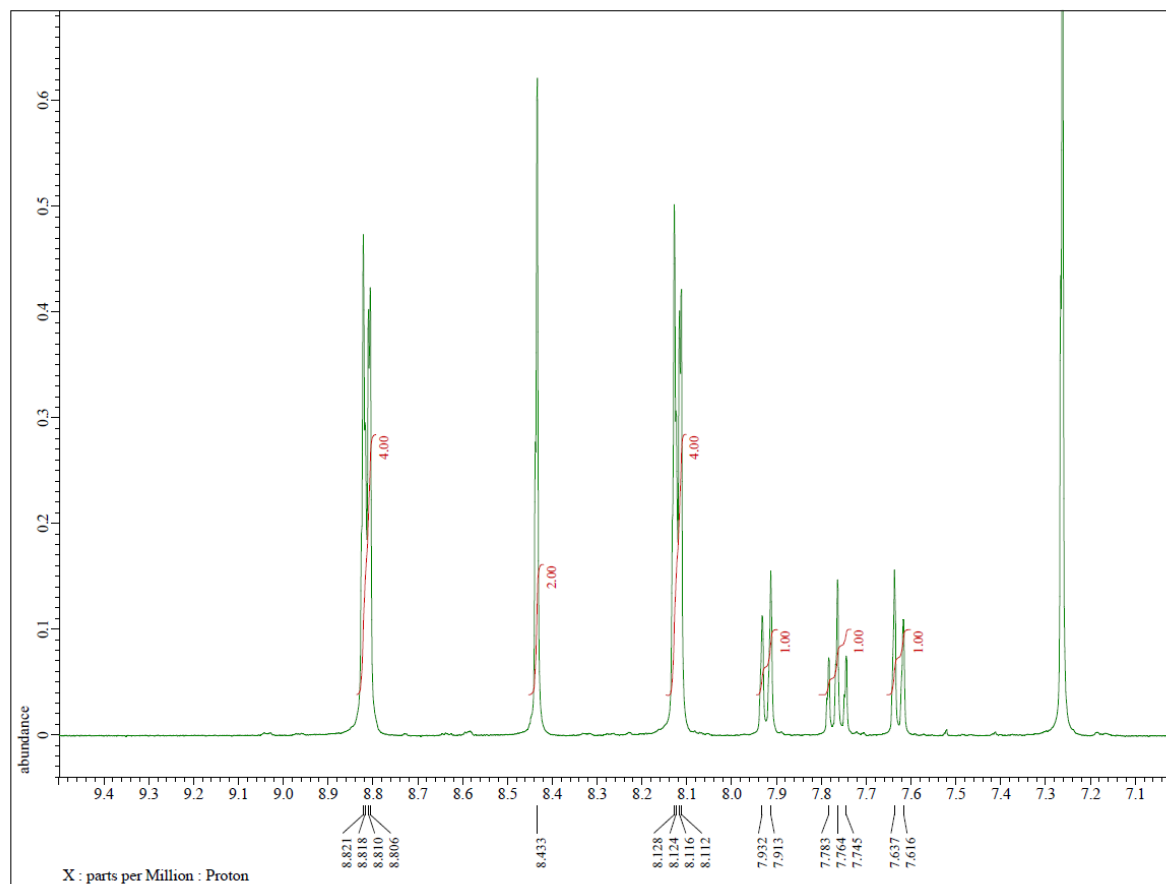
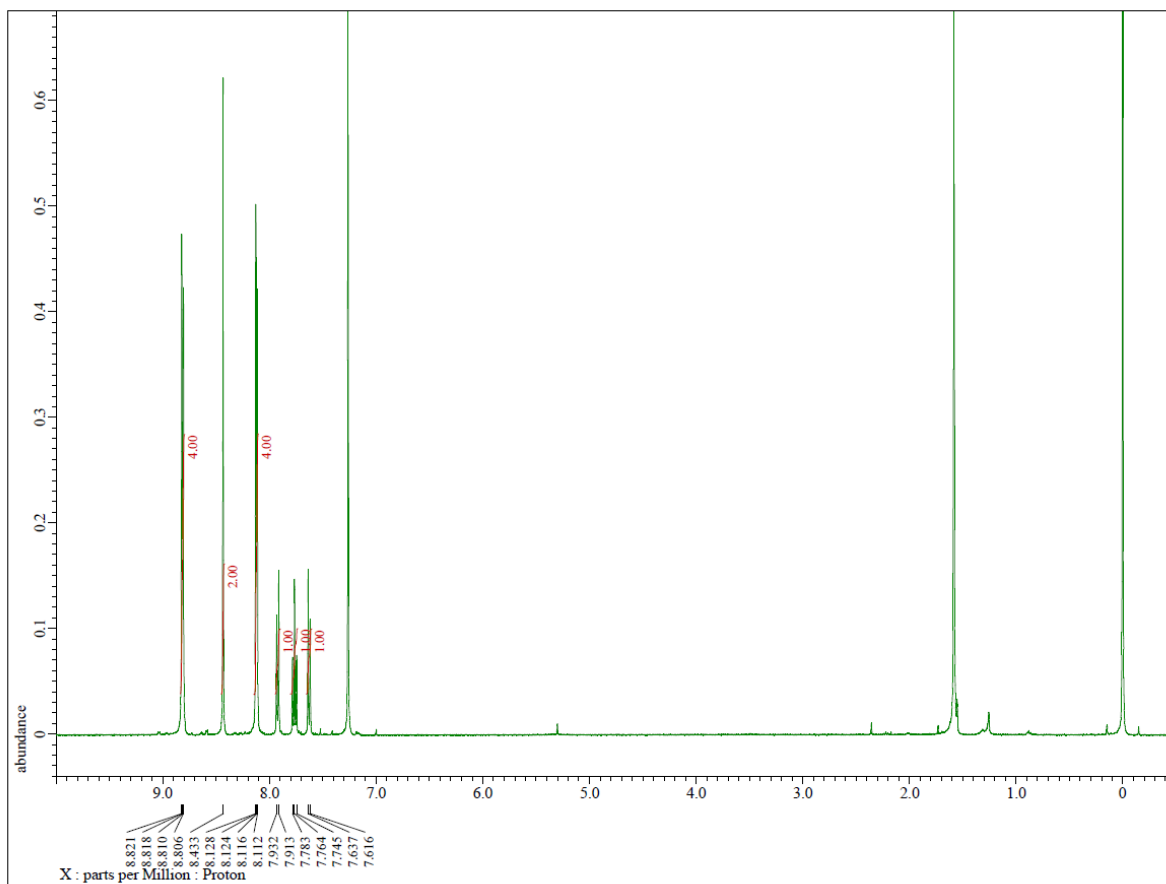


Figure S4. ^1H -NMR spectrum of TPy44PyBr (400 MHz, CDCl_3 , @R.T.)

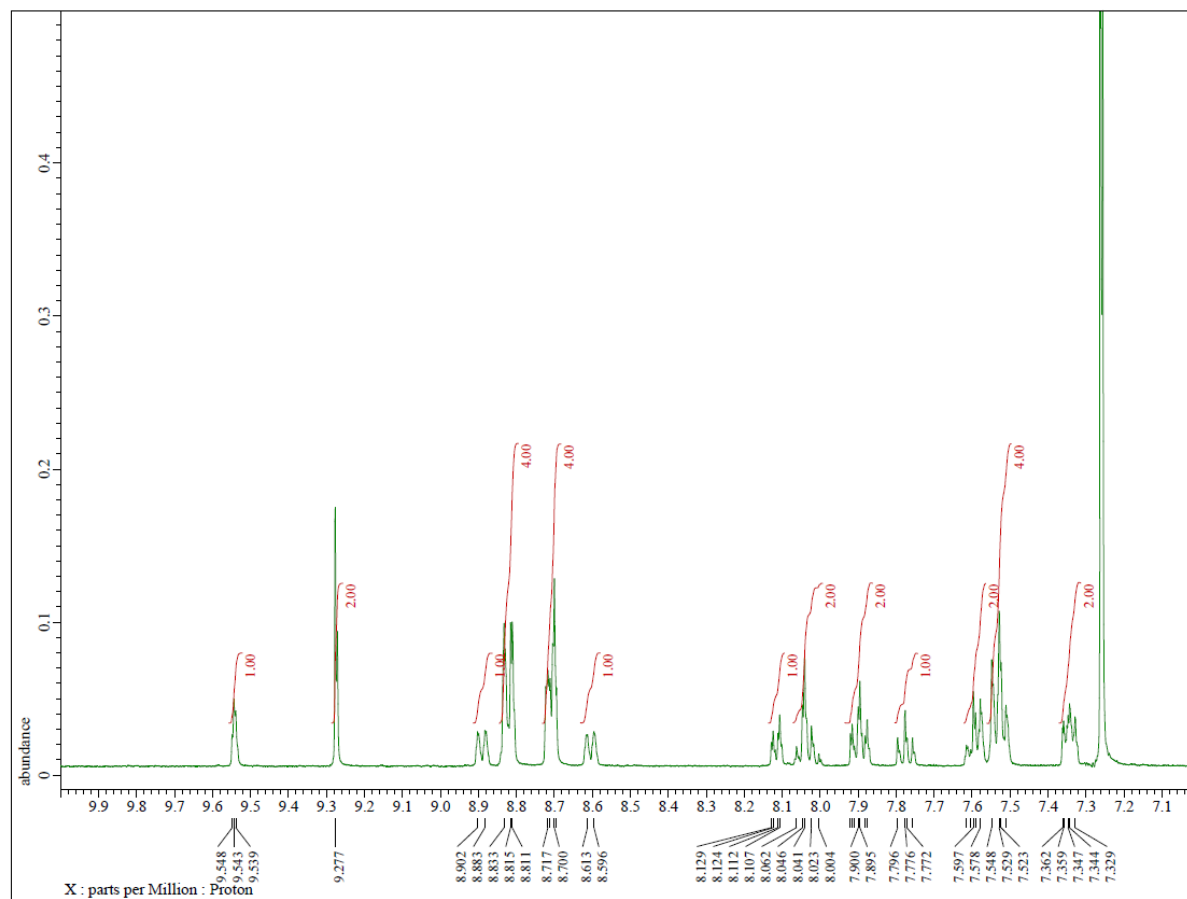
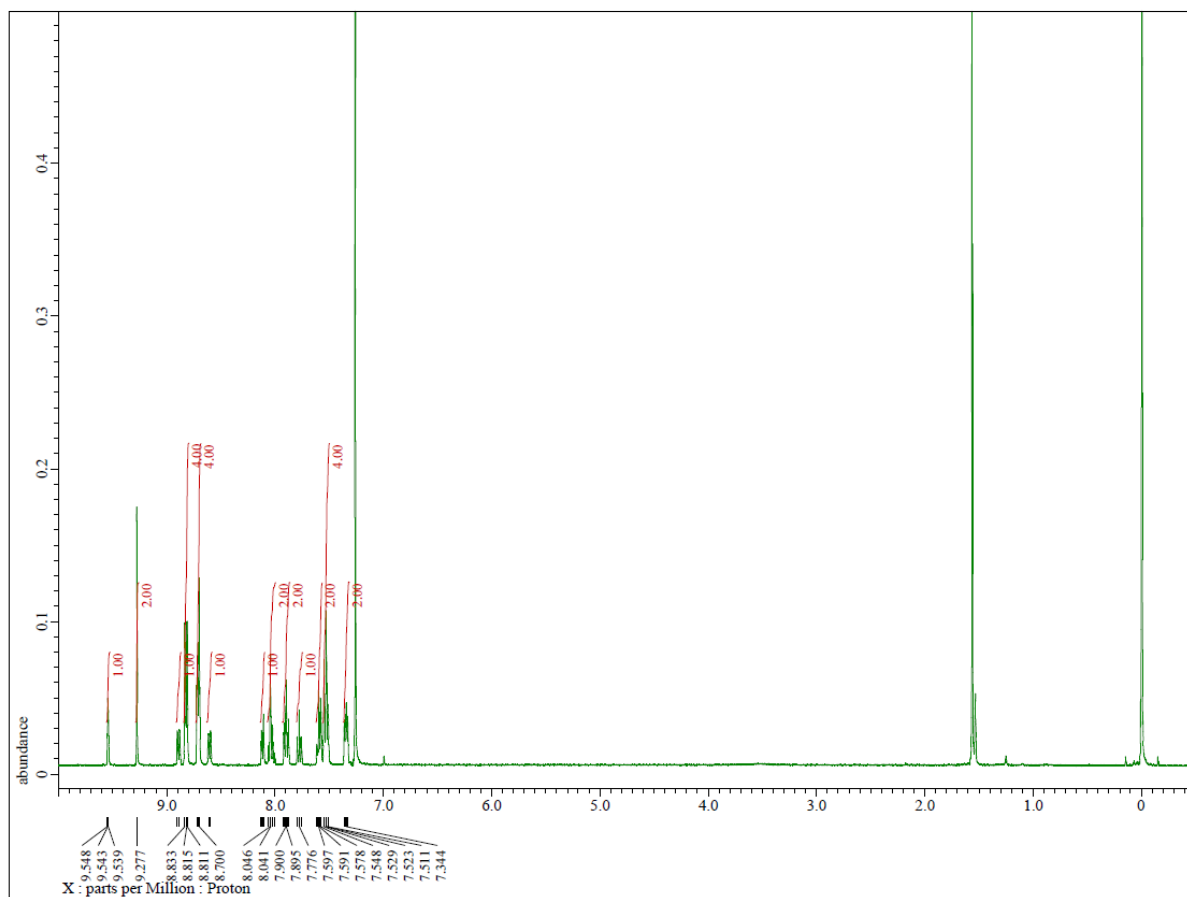


Figure S5. $^1\text{H-NMR}$ spectrum of T2PyTRZ (400 MHz, CDCl_3 , @R.T.)

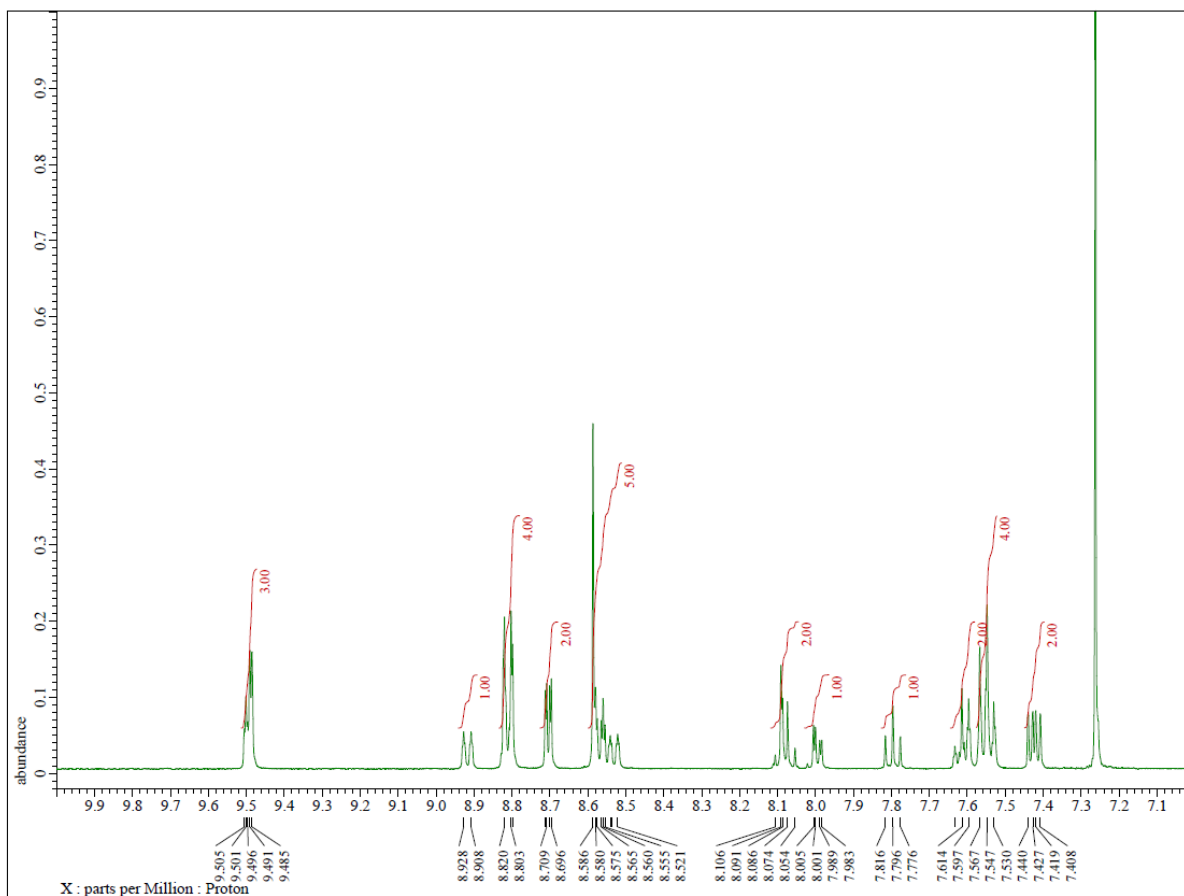
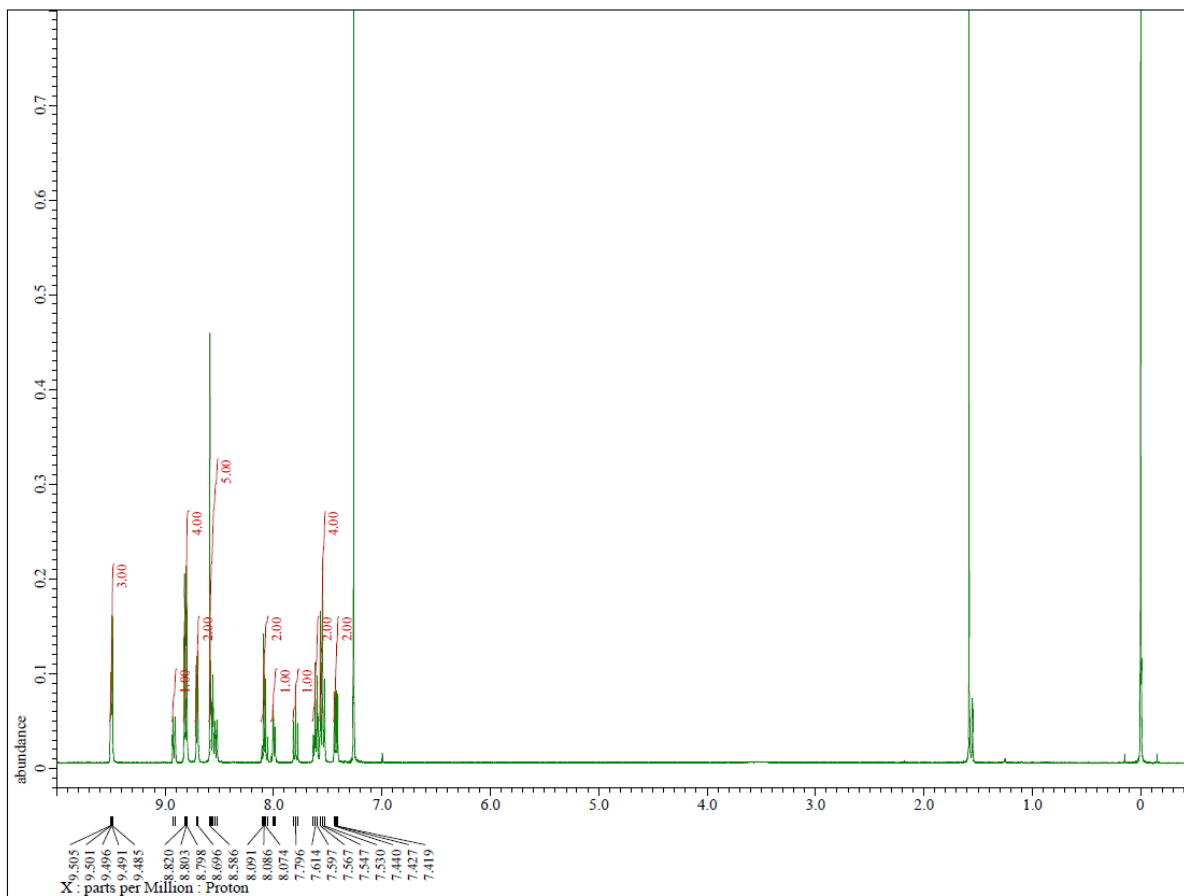


Figure S6. ¹H-NMR spectrum of T3PyTRZ (400 MHz, CDCl₃, @R.T.)

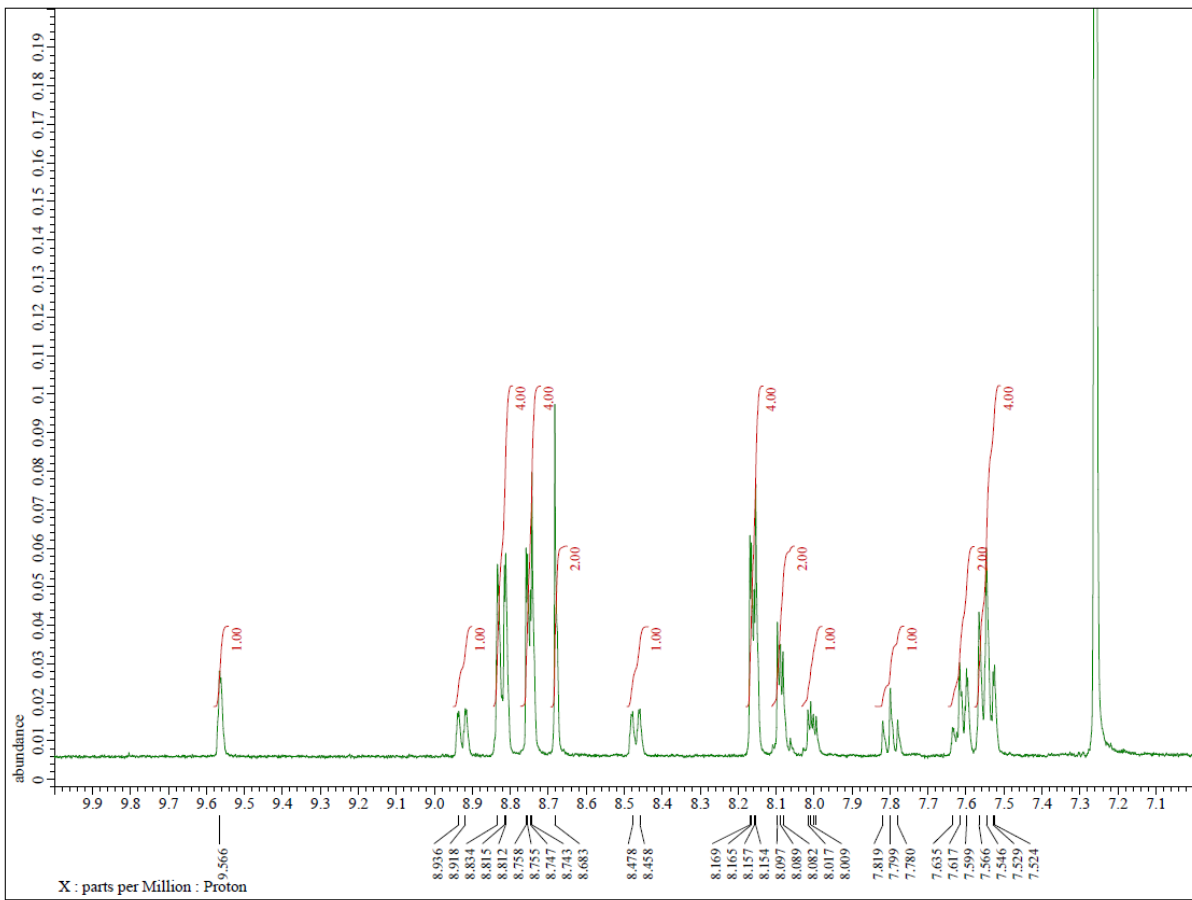
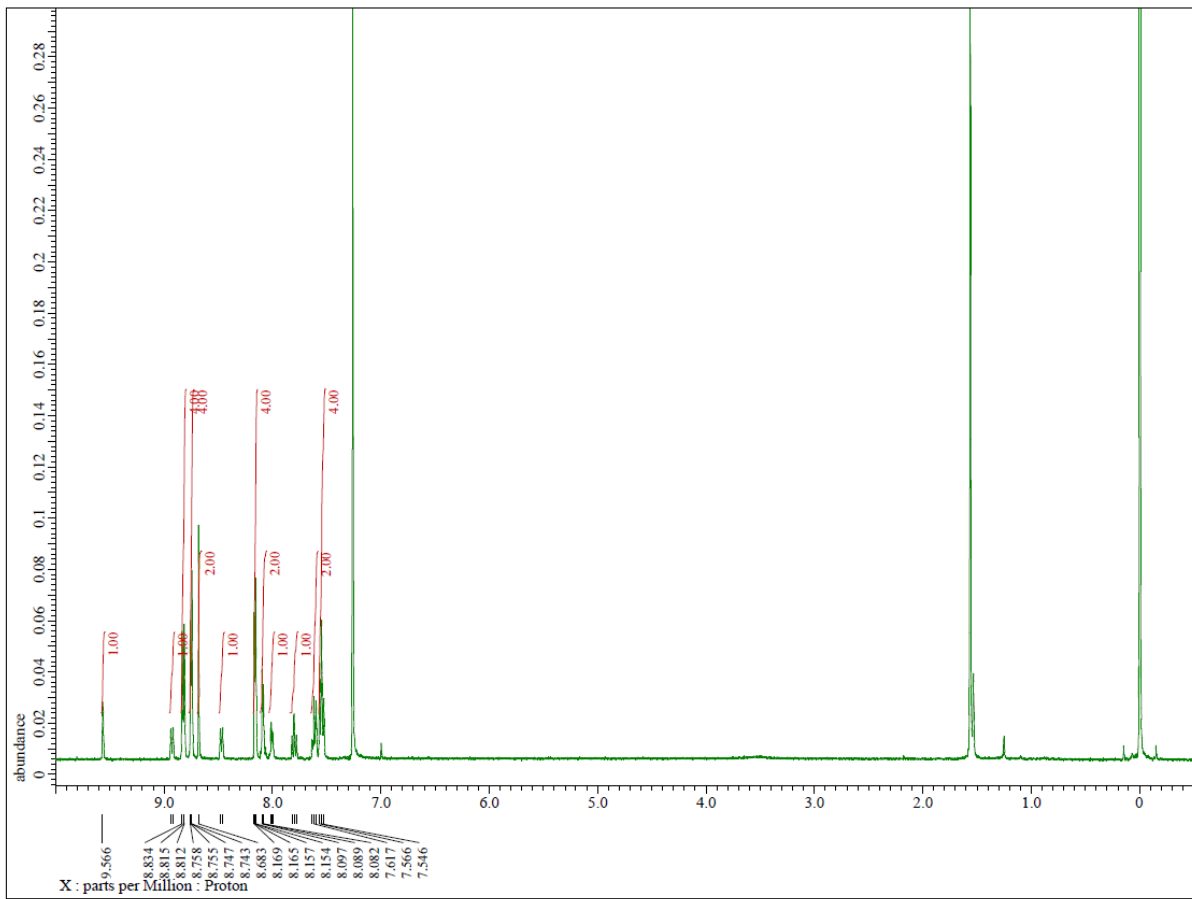


Figure S7. ¹H-NMR spectrum of T4PyTRZ (400 MHz, CDCl₃, @R.T.)

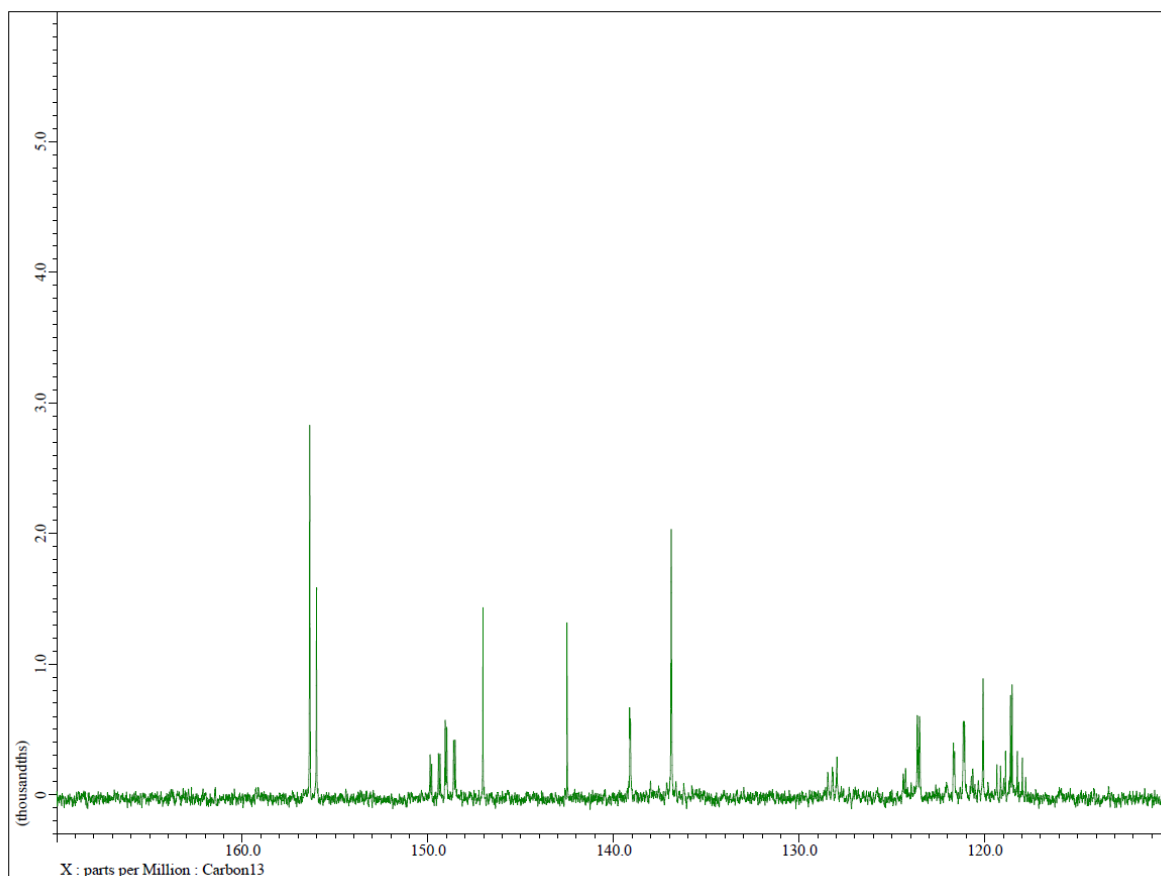
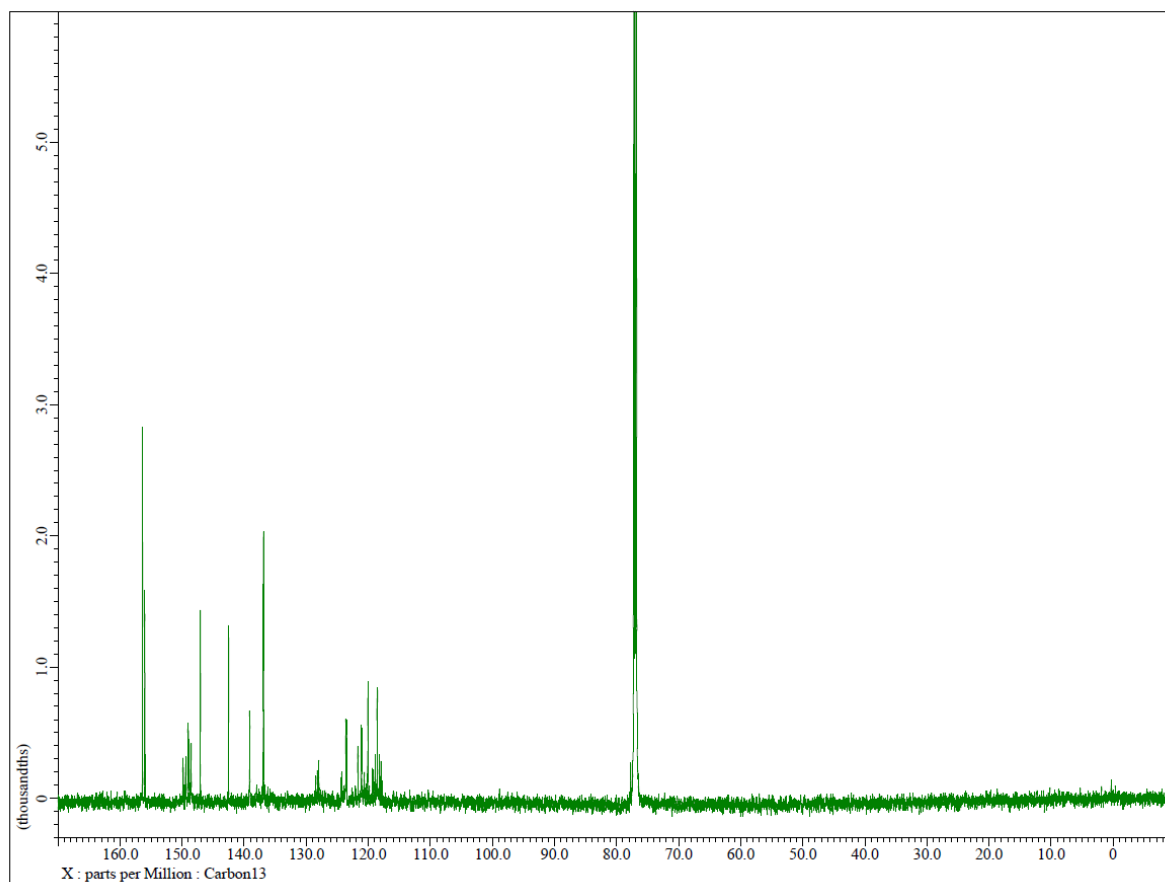


Figure S8. ^{13}C -NMR spectrum of TPy22PyBr (151 MHz, CDCl_3 , @R.T.)

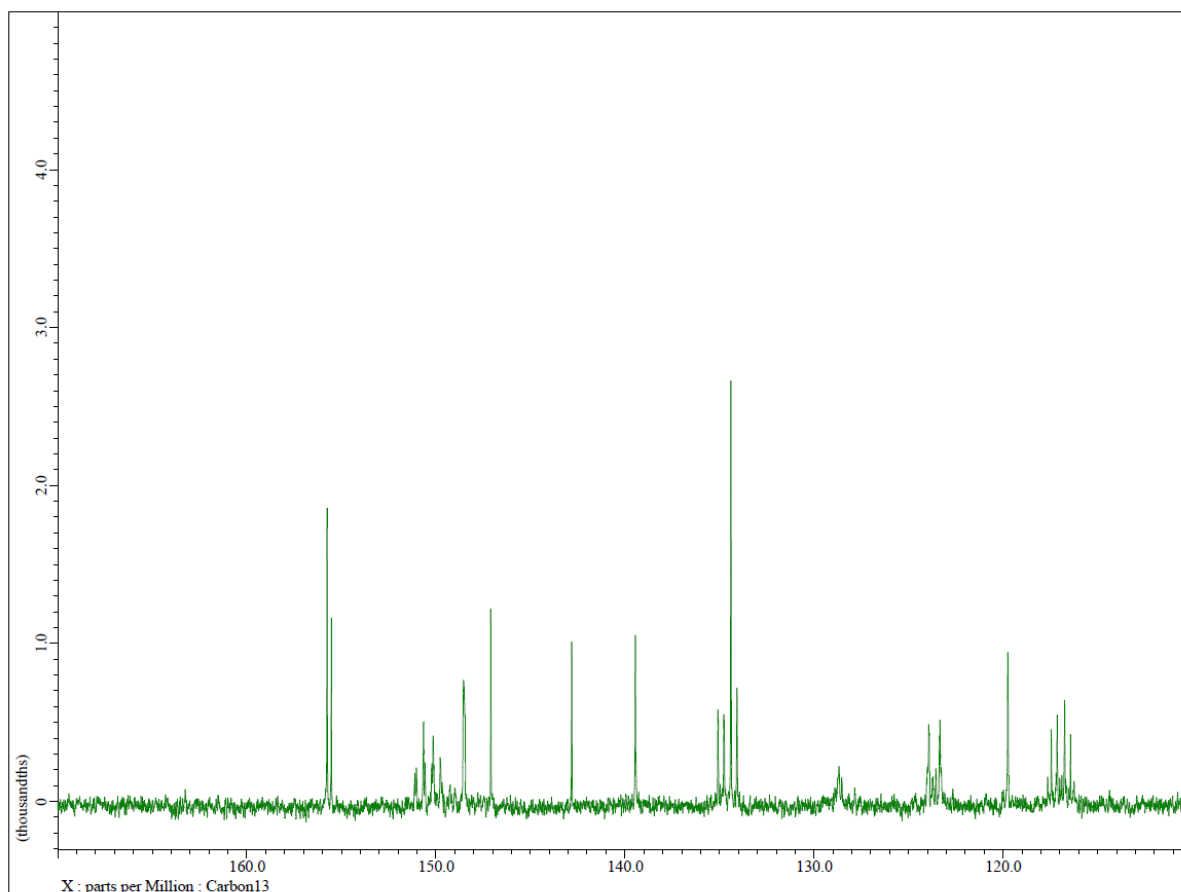
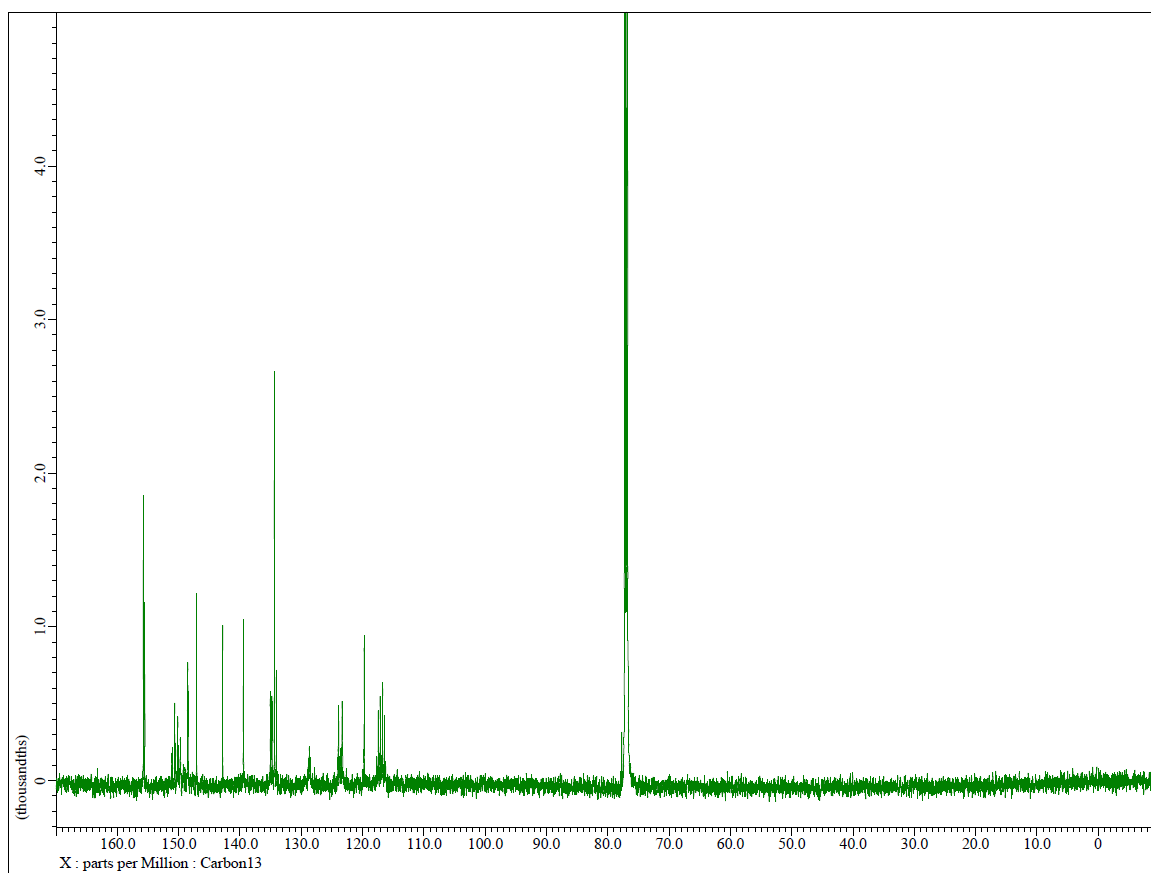


Figure S9. ¹³C-NMR spectrum of TPy33PyBr (151 MHz, CDCl₃, @R.T.)

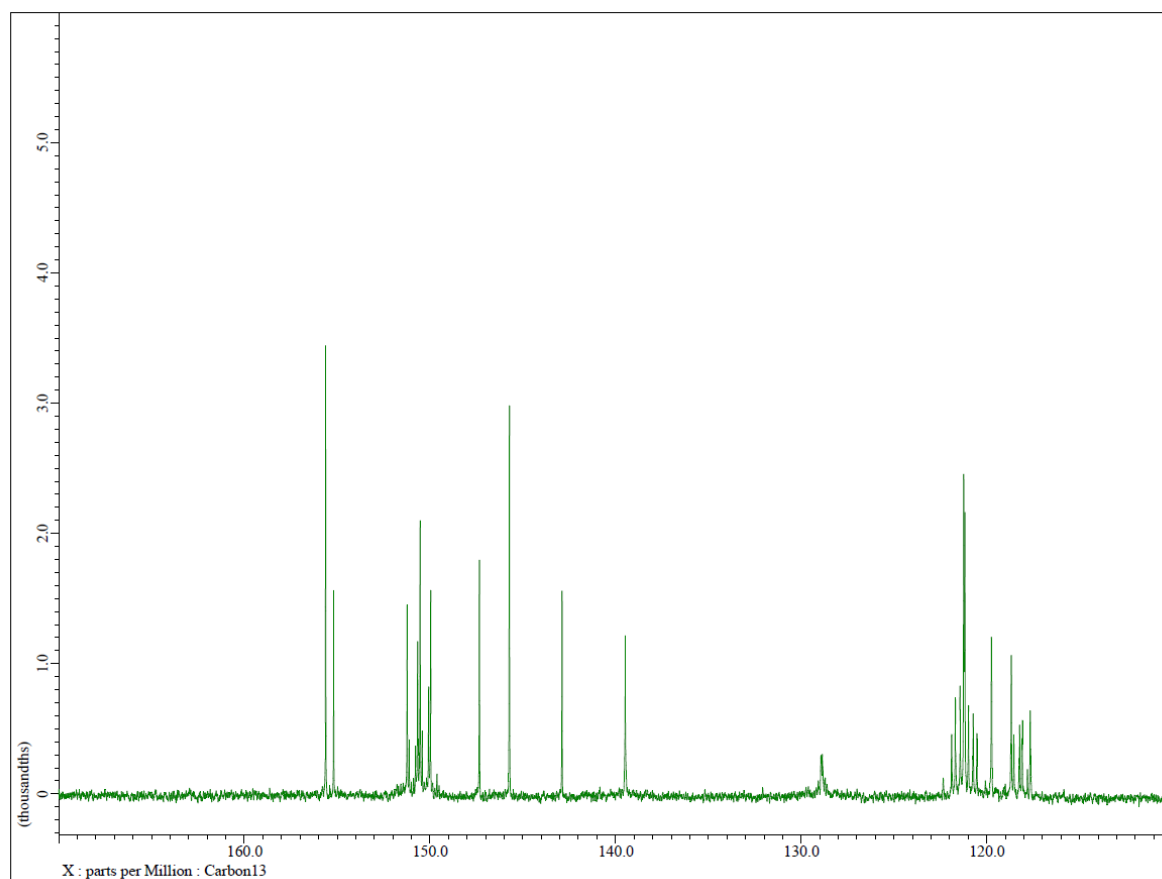
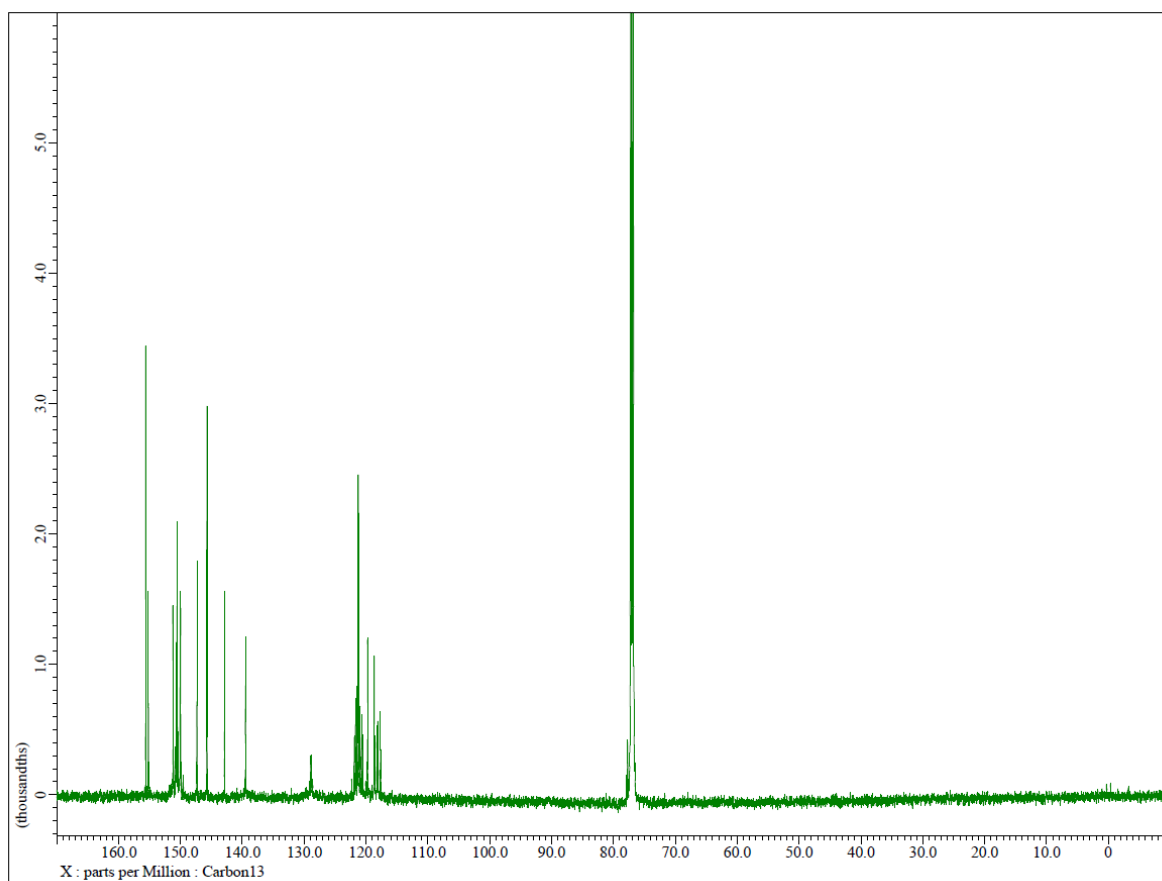


Figure S10. ^{13}C -NMR spectrum of TPY44PyBr (151 MHz, CDCl_3 , @R.T.)

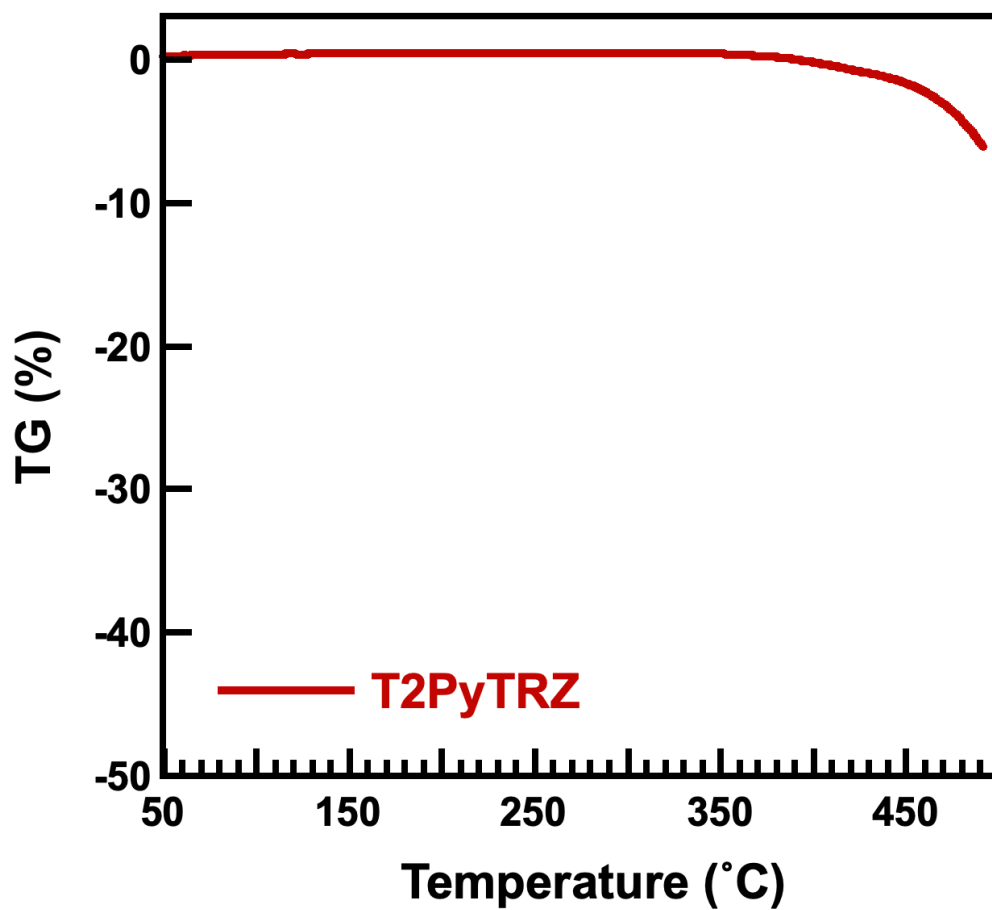


Figure S11. TGA thermogram of T2PyTRZ.

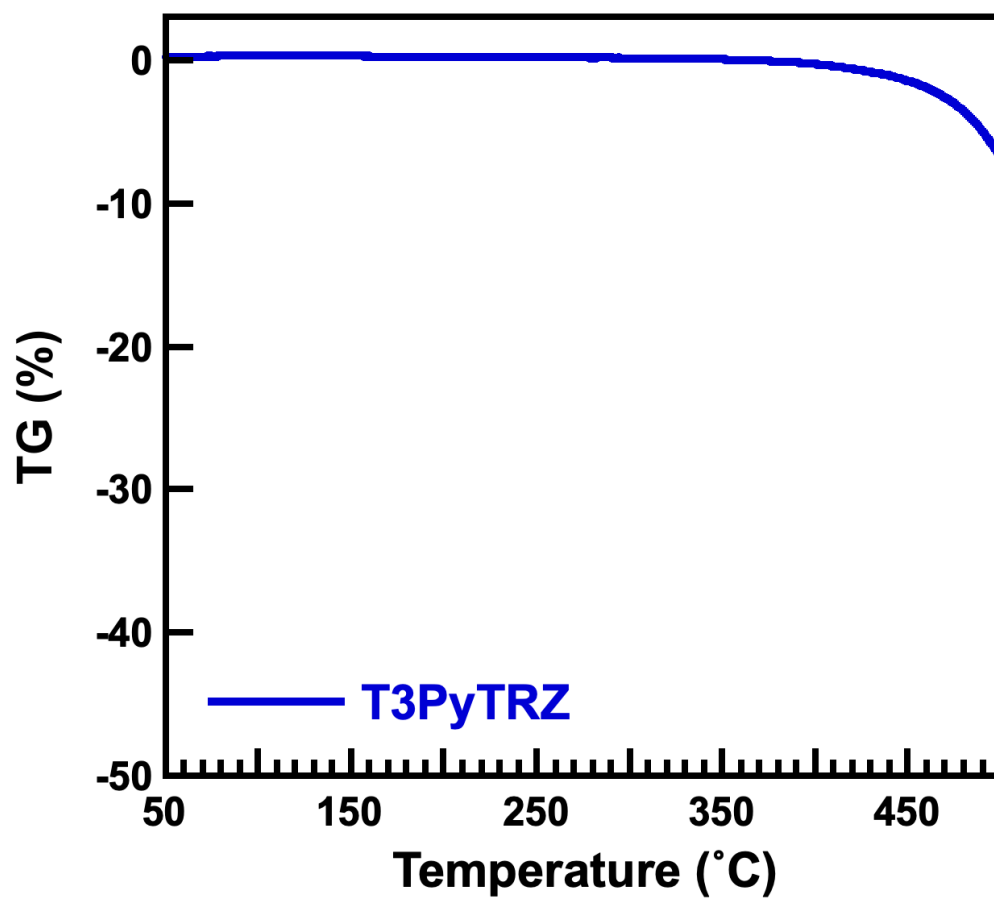


Figure S12. TGA thermogram of T3PyTRZ.

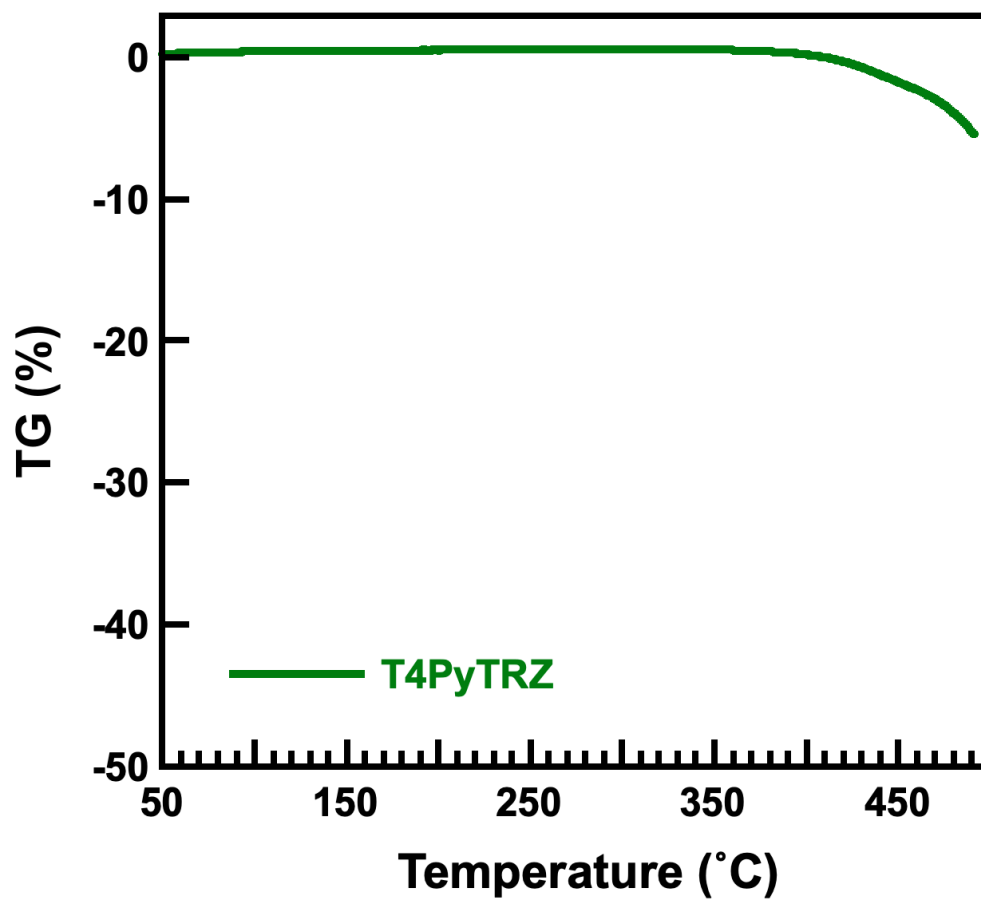


Figure S13. TGA thermogram of T4PyTRZ.

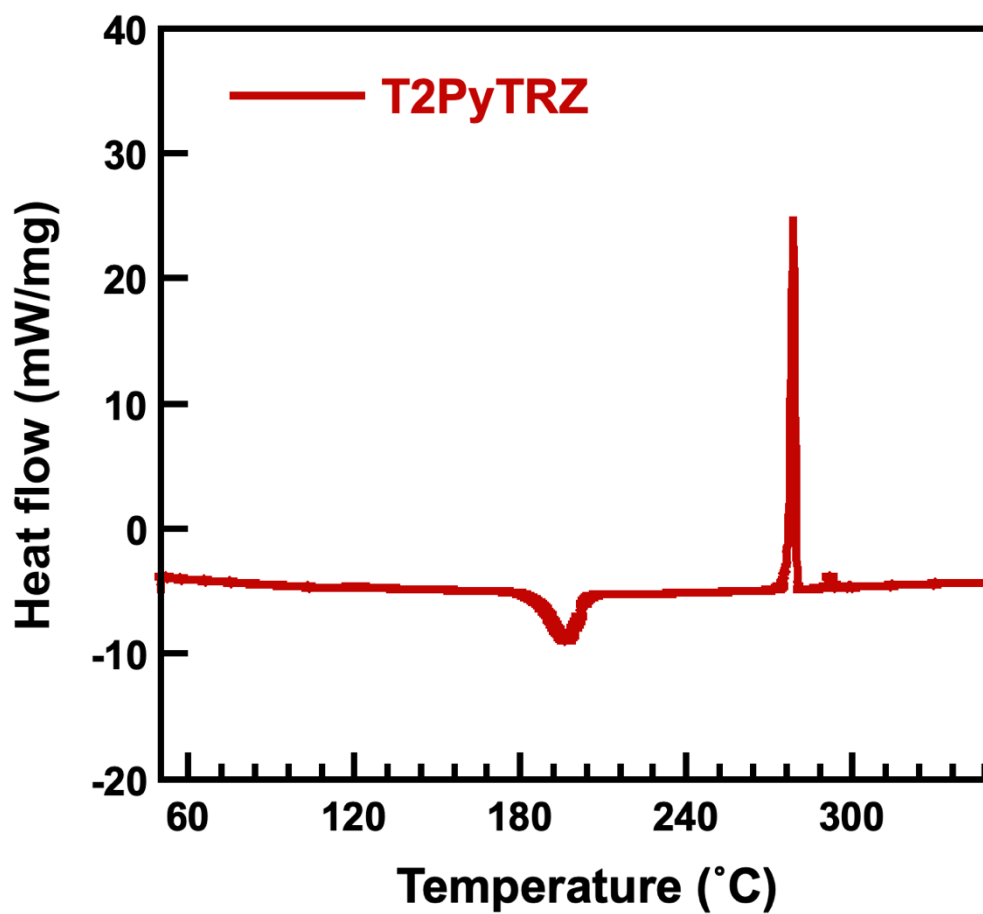


Figure S14. DSC curve of T2PyTRZ.

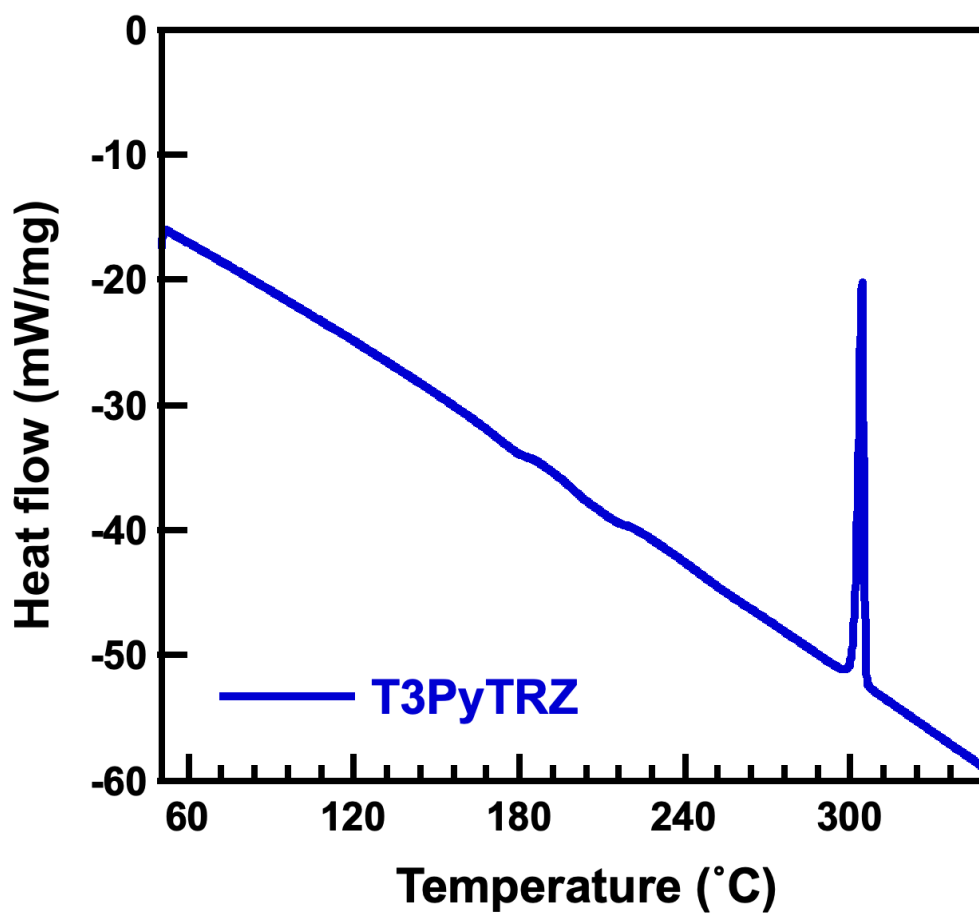


Figure S15. DSC curve of T3PyTRZ.

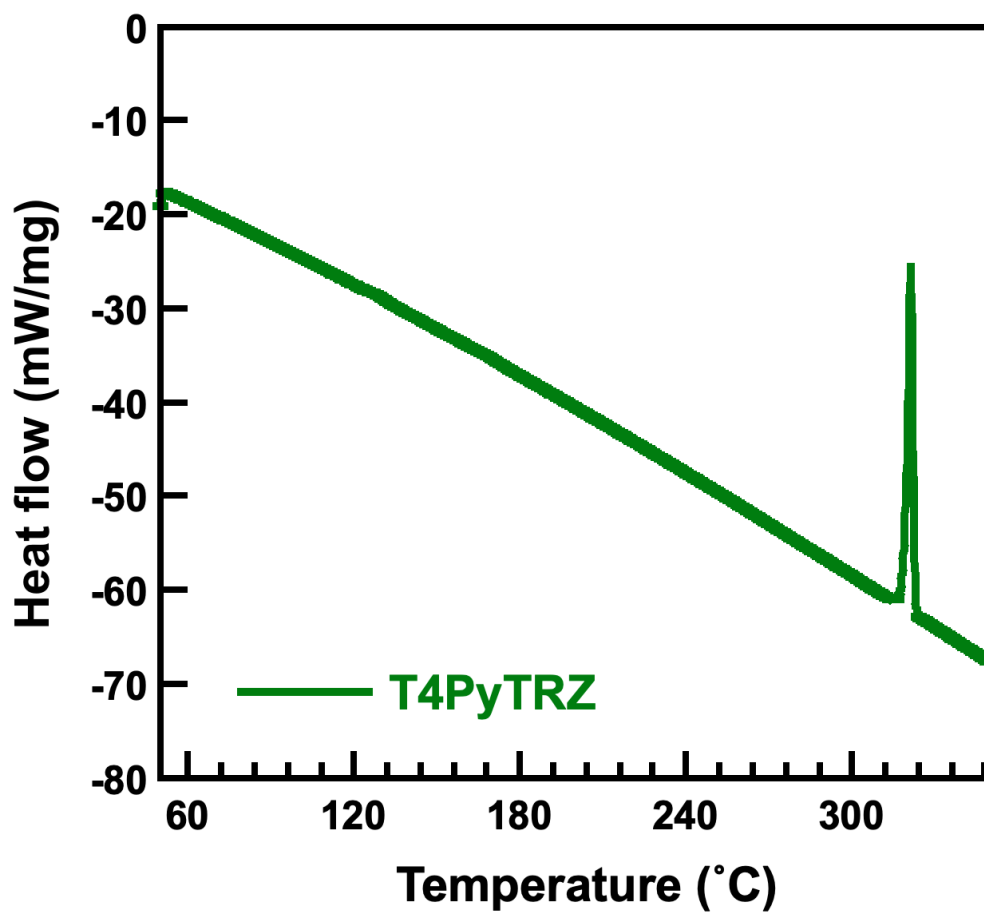


Figure S16. DSC curve of T4PyTRZ.

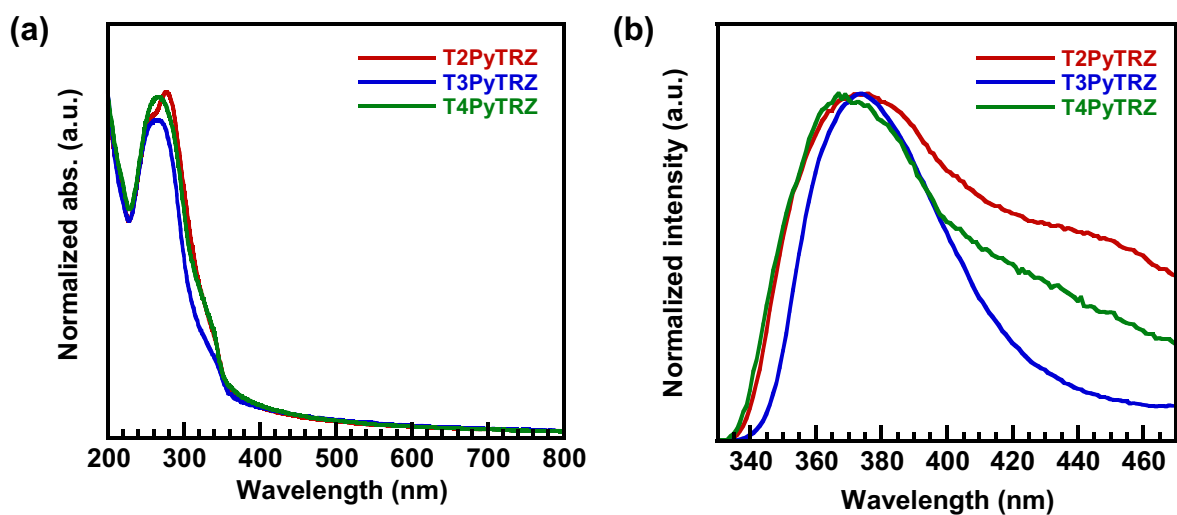


Figure S17. (a) Normalized UV-vis absorption and (b) normalized PL spectra of the **T_nPyTRZ** derivatives in vacuum deposited films.

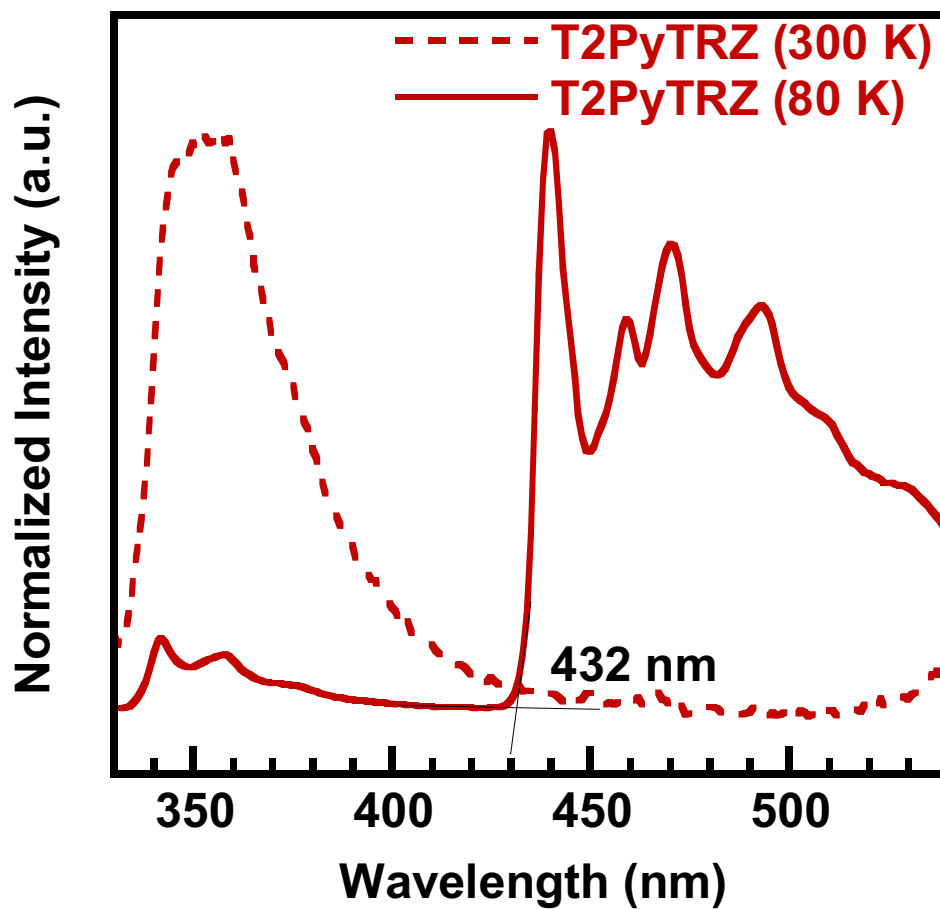


Figure S18. PL spectra in 2-methyltetrahydrofuran solution of T2PyTRZ at 300 K (excited at 300 nm) and 80 K (excited at 300 nm).

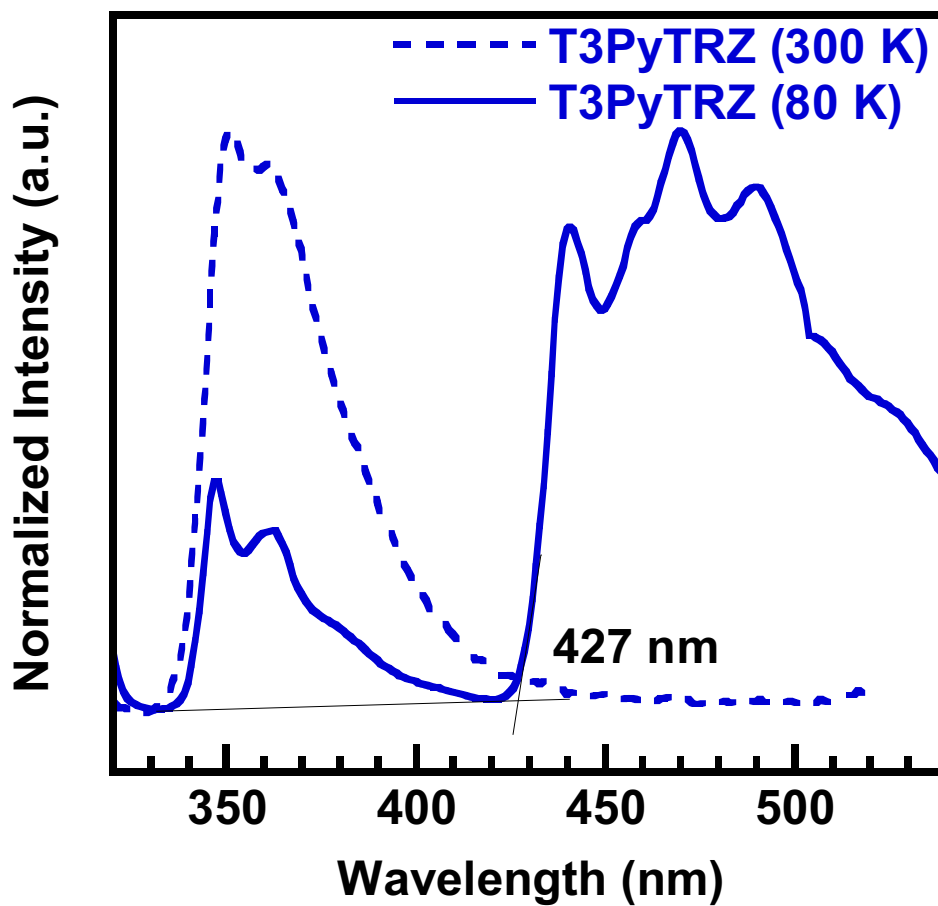


Figure S19. PL spectra in 2-methyltetrahydrofuran solution of T3PyTRZ at 300 K (excited at 290 nm) and 80 K (excited at 300 nm).

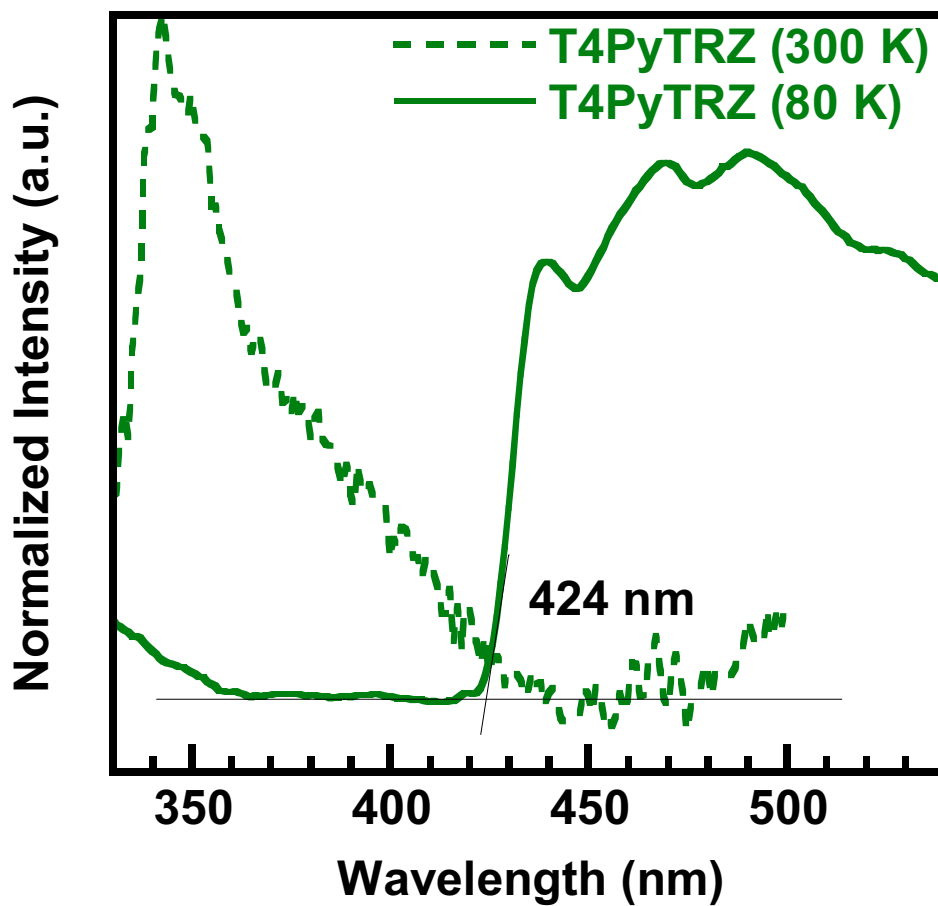


Figure S20. PL spectra in 2-methyltetrahydrofuran solution of T4PyTRZ at 300 K (excited at 290 nm) and 80 K (excited at 300 nm).

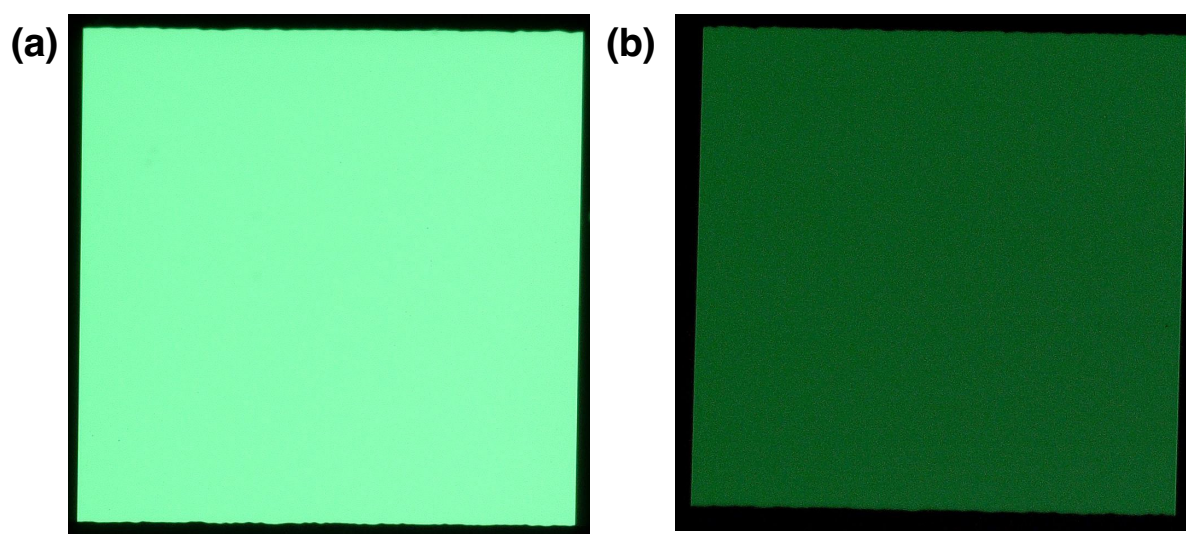


Figure S21. Photographs of the encapsulated T2PyTRZ-based OLED (a) before and (b) after the stability test at 5.4 V.

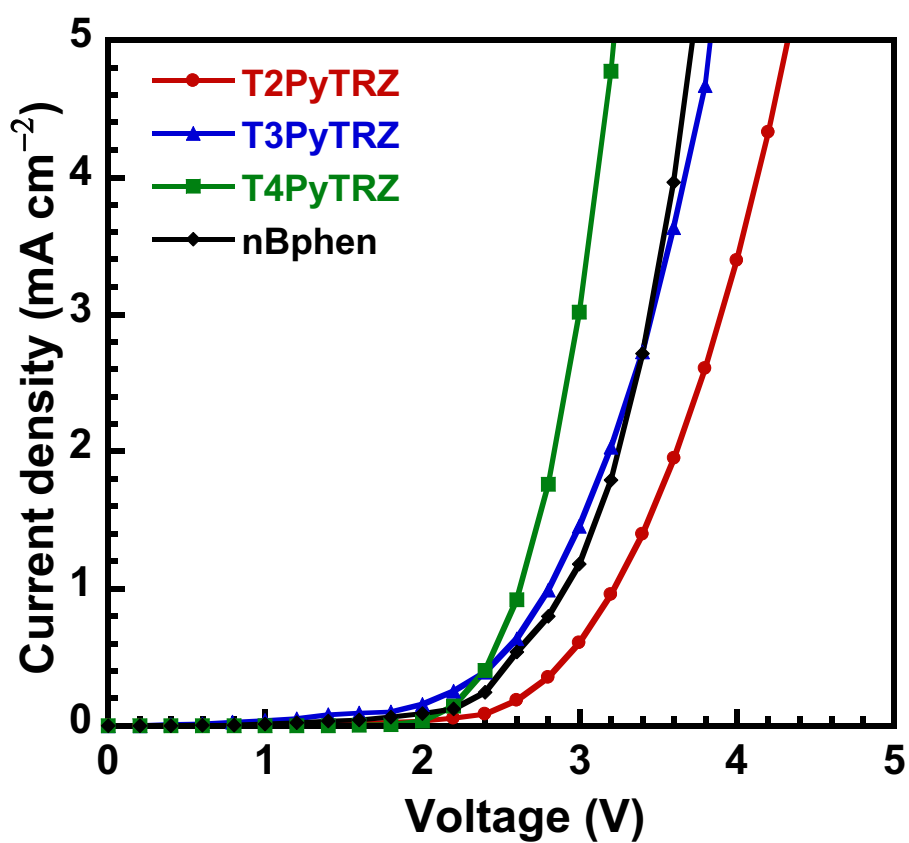


Figure S22. The current density–voltage characteristics of electron-only devices with the structure of [ITO/ETL (100 nm)/Liq (1 nm)/Al].